united nations
educational, scientific
and cultural
organization

international atomic
energy agency

the
abdus salam
international centre for theoretical physics

SMR.1303 - 3

Advanced Course:
CLIMATE CHANGE IN THE MEDITERRANEAN REGION
PART I: PHYSICAL ASPECTS
(12 - 16 March 2001)

"Effects on Climate of Greenhouse Gases Concentrations"

Serge PLANTON
Meteo-France Centre National de Recherches Meteorologiques
CNRM / GMGEC
42 Avenue G. Coriolis
F-31057 Toulouse cedex 01
FRANCE

Effects on climate of greenhouse gases concentrations

1. Introduction

2. The greenhouse effect

3. Observed climate change

4. Projected climate change

1. Introduction

- Observed and projected climate change are successively examined at the global scale and over the Mediterranean region.

- Presented illustrations are mainly coming from the IPCC Working Group I reports and from the results of specific research projects.

  The IPCC was established by the World Meteorological Organisation (WMO) and the United Nations Environment Programme (UNEP) in 1988 to provide an assessment of the understanding on climate change due to natural and anthropogenic forcing. The Working group I addresses the scientific aspects of climate change.

  Research projects are aimed at identifying the main climate processes and feedbacks playing a role in climate change, at detecting climate change and attributing it to human activities, at constructing climate change scenarios.

2. The greenhouse effect

- Natural origin

Due to the absorption of infrared radiation by gases such as water vapour, carbon dioxide, nitrous oxide, methane, ozone.

Radiative forcing due to greenhouse gases implies a warming of near 33°C of the equilibrium surface temperature.

- Anthropogenic

Due to the human-induced increase of greenhouse gases concentrations such as above mentioned gases and Halocarbons.

Radiative forcing due to greenhouse exceeds radiative forcing due to human-induced changes of aerosols concentrations and due to natural sources of climate variability (sun, volcanoes).

Anthropogenic greenhouse gases concentrations increase may have a significant influence on climate that need to be investigated.

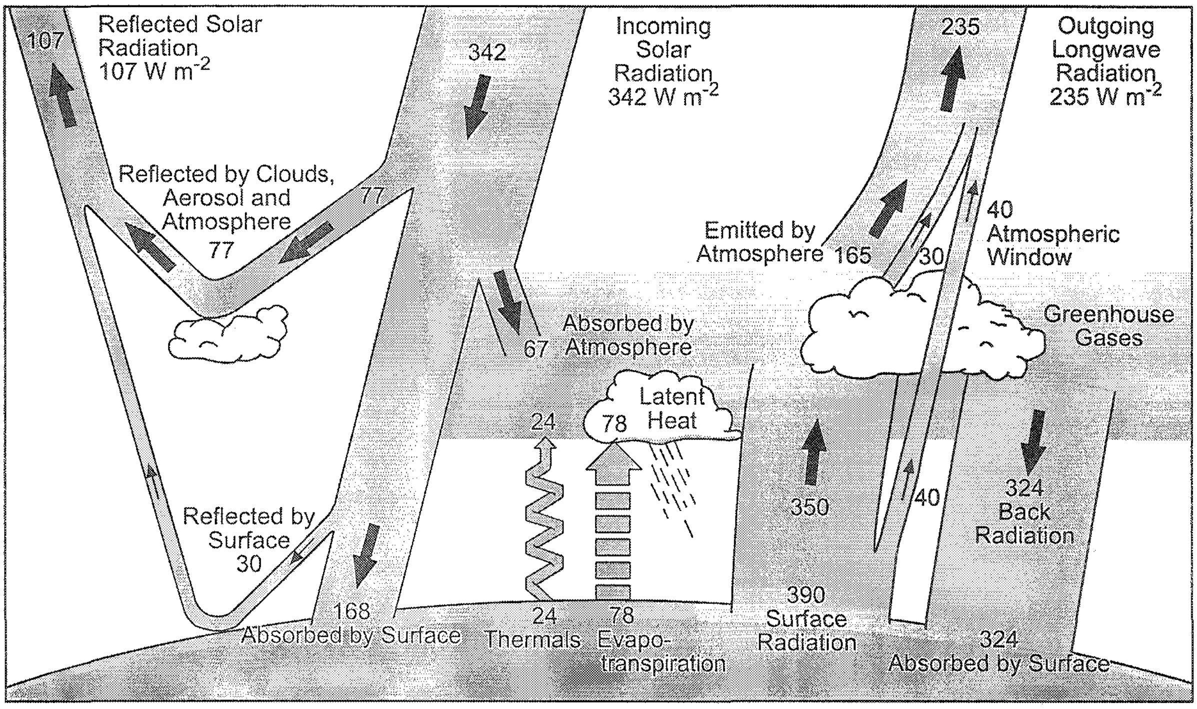

Figure 1.2: The Earth's annual and global mean energy balance. Of the incoming solar radiation, 49% (168 Wm^{-2}) is absorbed by the surface. That heat is returned to the atmosphere as sensible heat, as evapotranspiration (latent heat) and as thermal infrared radiation. Most of this radiation is absorbed by the atmosphere, which in turn emits radiation both up and down. The radiation lost to space comes from cloud tops and atmospheric regions much colder than the surface. This causes a greenhouse effect. Source: Kiehl and Trenberth, 1997.

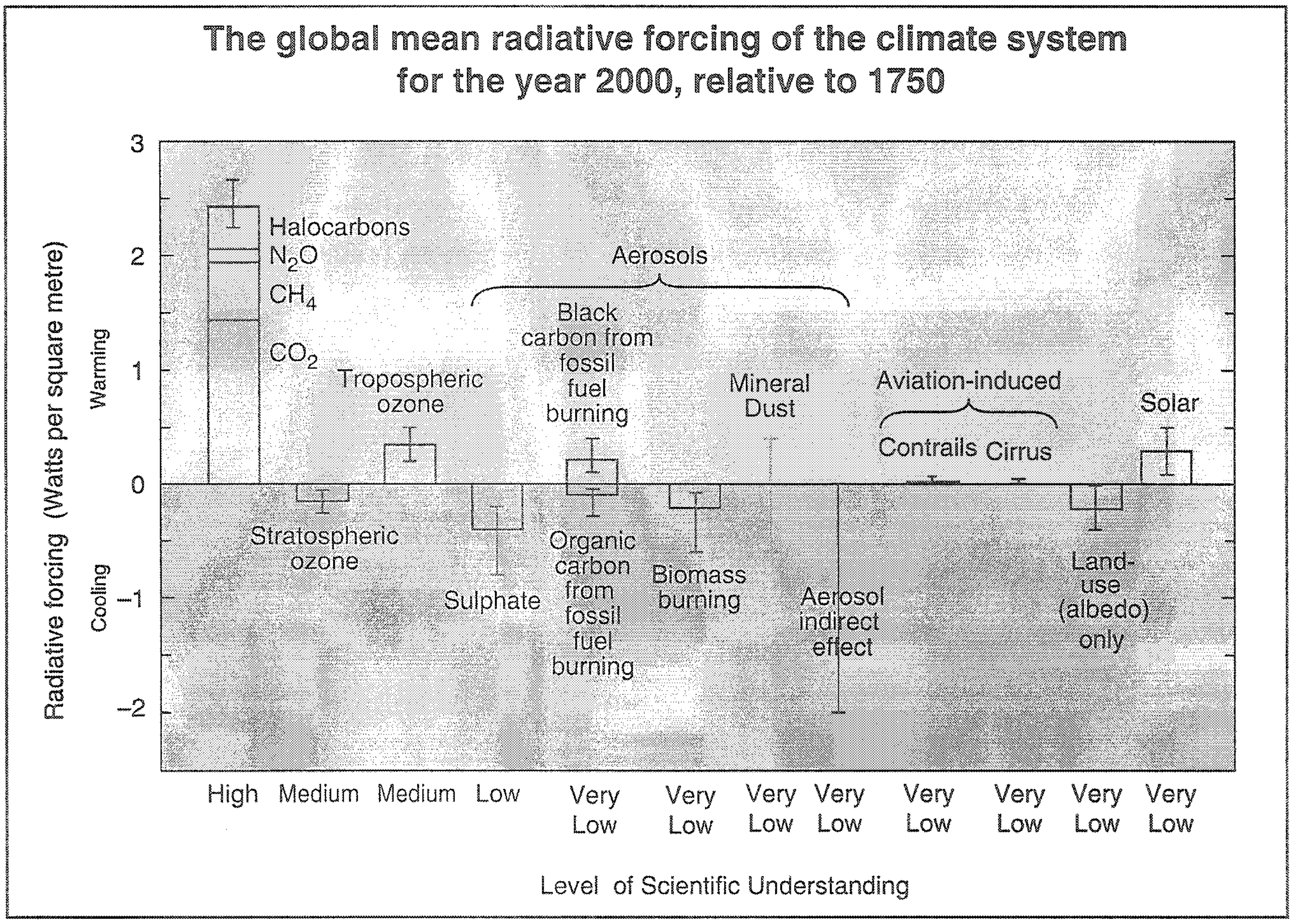

Figure 3: Many external factors force climate change.

These radiative forcings arise from changes in the atmospheric composition, alteration of surface reflectance by land use, and variation in the output of the sun. Except for solar variation, some form of human activity is linked to each. The rectangular bars represent estimates of the contributions of these forcings – some of which yield warming, and some cooling. Forcing due to episodic volcanic events, which lead to a negative forcing lasting only for a few years, is not shown. The indirect effect of aerosols shown is their effect on the size and number of cloud droplets. A second indirect effect of aerosols on clouds, namely their effect on cloud lifetime, which would also lead to a negative forcing, is not shown. Effects of aviation on greenhouse gases are included in the individual bars. The vertical line about the rectangular bars indicates a range of estimates, guided by the spread in the published values of the forcings and physical understanding. Some of the forcings possess a much greater degree of certainty than others. A vertical line without a rectangular bar denotes a forcing for which no best estimate can be given owing to large uncertainties. The overall level of scientific understanding for each forcing varies considerably, as noted. Some of the radiative forcing agents are well mixed over the globe, such as CO_2, thereby perturbing the global heat balance. Others represent perturbations with stronger regional signatures because of their spatial distribution, such as aerosols. For this and other reasons, a simple sum of the positive and negative bars cannot be expected to yield the net effect on the climate system. The simulations of this assessment report (for example, Figure 5) indicate that the estimated net effect of these perturbations is to have warmed the global climate since 1750. [Based upon Chapter 6, Figure 6.6]

Figures

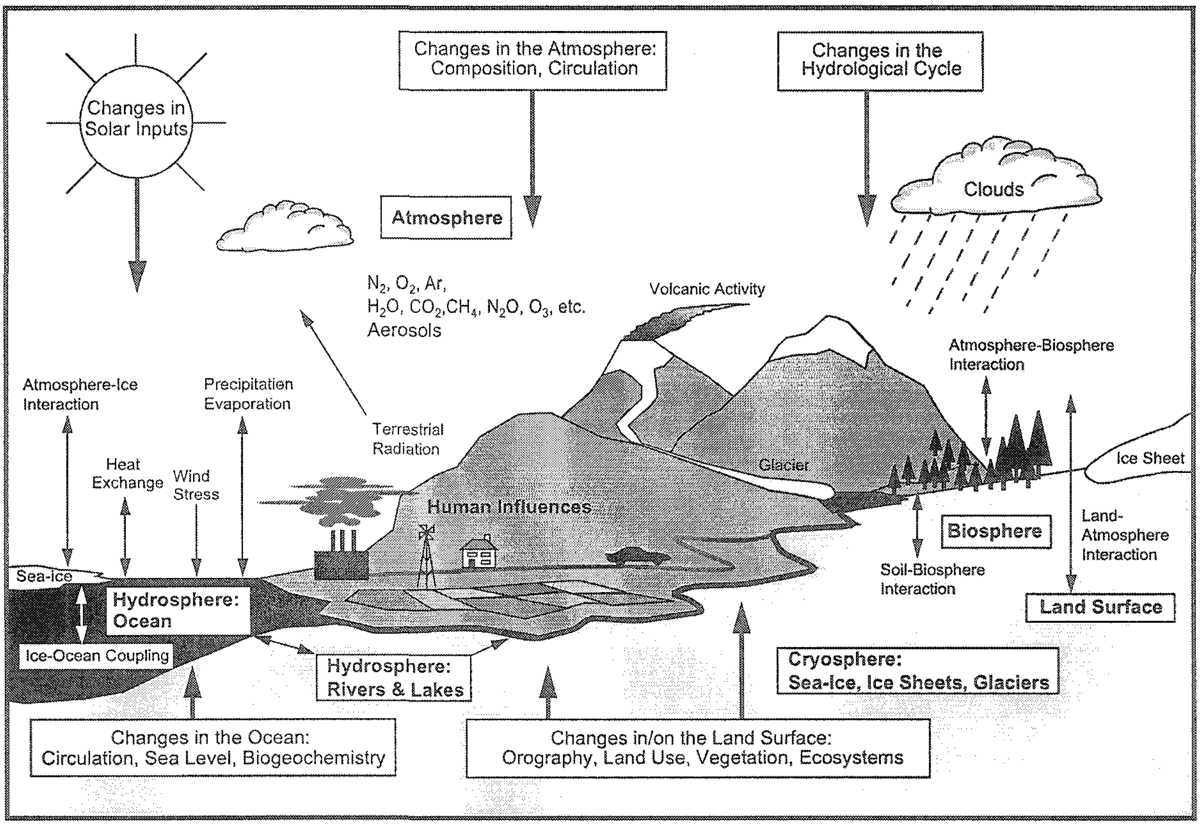

Figure 1.1: Schematic view of the components of the global climate system (bold), their processes and interactions (thin arrows) and some aspects that may change (bold arrows).

3. Observed climate change

The data sources

- "Proxy" and paleoclimatical data

  Indicators from ice cores, tree rings, corals, ... related to climate parameters.

  → Antarctic temperature reconstruction over the last 420000 years from Vostok ice core (Petit et al,1999).

  → Northern Hemisphere temperature reconstruction over the past millennium (Mann et al,1995).

- Instrumental data

  Meteorological parameters measured at land stations or onboard ships since the middle of 19^{th} century

  → Combined land-surface air temperature and sea surface anomalies (Folland et al, 2000).

  → Climatology of temperature and precipitation of (Legates and Willmott,1990).

  → Climate Atlas of ECSN : « Climate of Europe » (1995).

3. Observed climate change

The data sources

- Satellite data

  Radiation measurement at various frequencies since the 60s.

  → Precipitation climatology of Xie et Arkin (1996).

- Reanalyses from weather forecast centres

  Reprocessing of instrumental and satellite data over a given period using the state of the art of a data assimilation system.

  → Reanalyse over 40 years from NCEP, over 15 years from CEPMMT ...

Precipitation Legates and Willmott (mm/day)

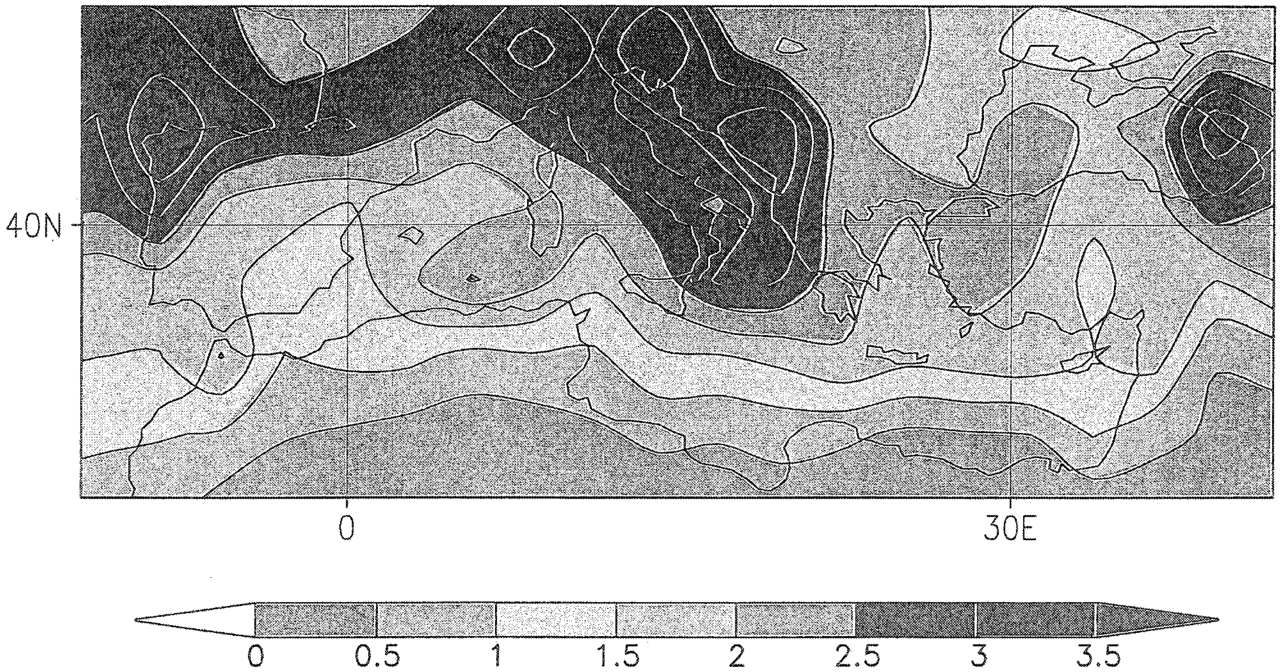

Precipitation CEP reanalysis (mm/day)

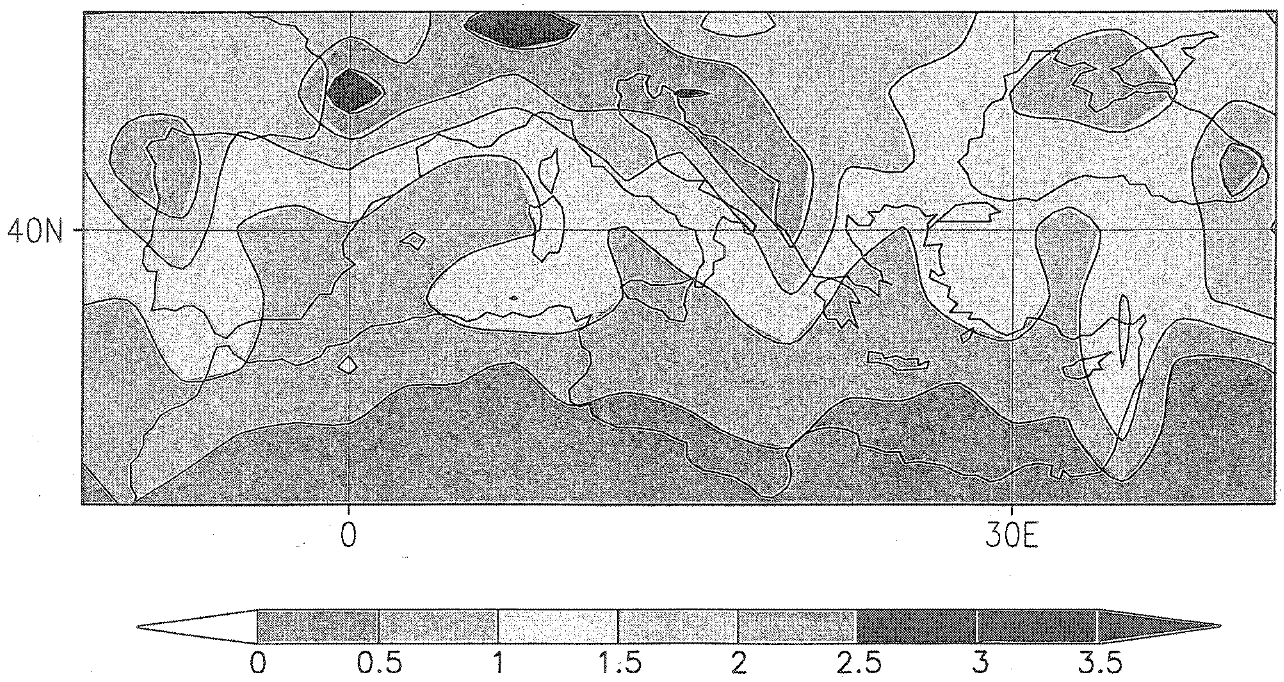

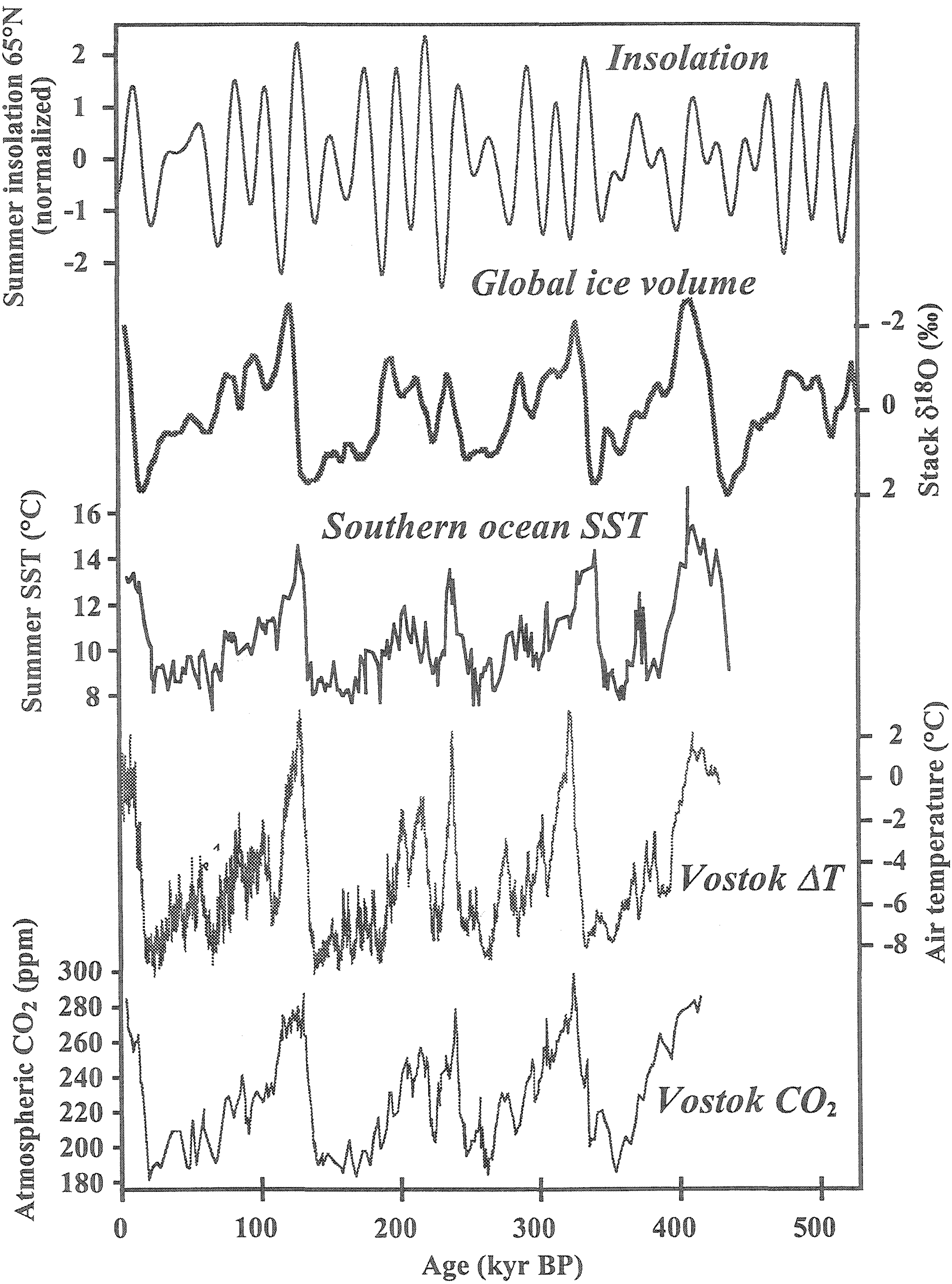
Insolation
Global ice volume
Southern ocean SST
Vostok ΔT
Vostok CO_2
Summer insolation 65°N (normalized)
2
1
0
-1
-2
Stack δ18O (‰)
-2
0
2
Summer SST (°C)
16
14
12
10
8
Air temperature (°C)
2
0
-2
-4
-6
-8
Atmospheric CO_2 (ppm)
300
280
260
240
220
200
180
0
100
200
300
400
500
Age (kyr BP)

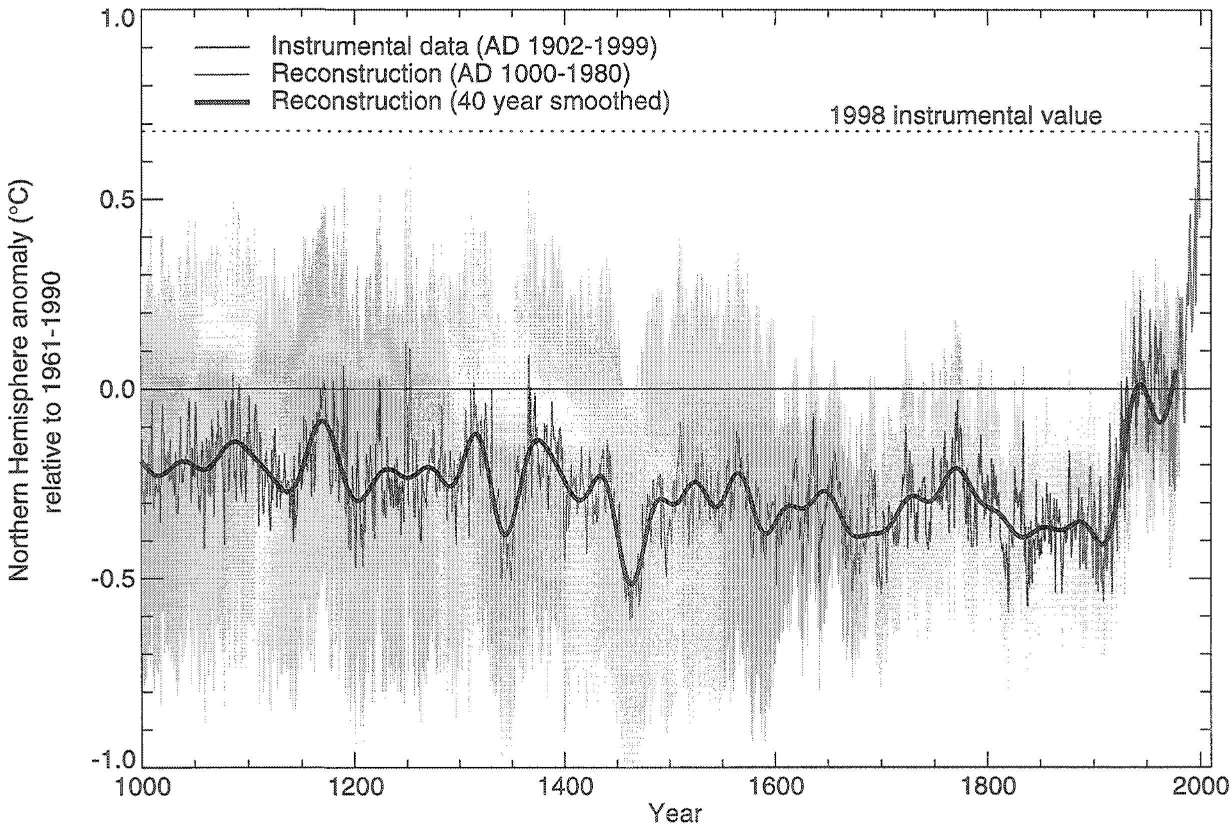

Figure 5: Millennial Northern Hemisphere (NH) temperature reconstruction (blue) and instrumental data (red) from AD 1000-1999. Smoother version of NH series (black), and two standard error limits (gray shaded) are shown. [Based on Figure 2.20.]

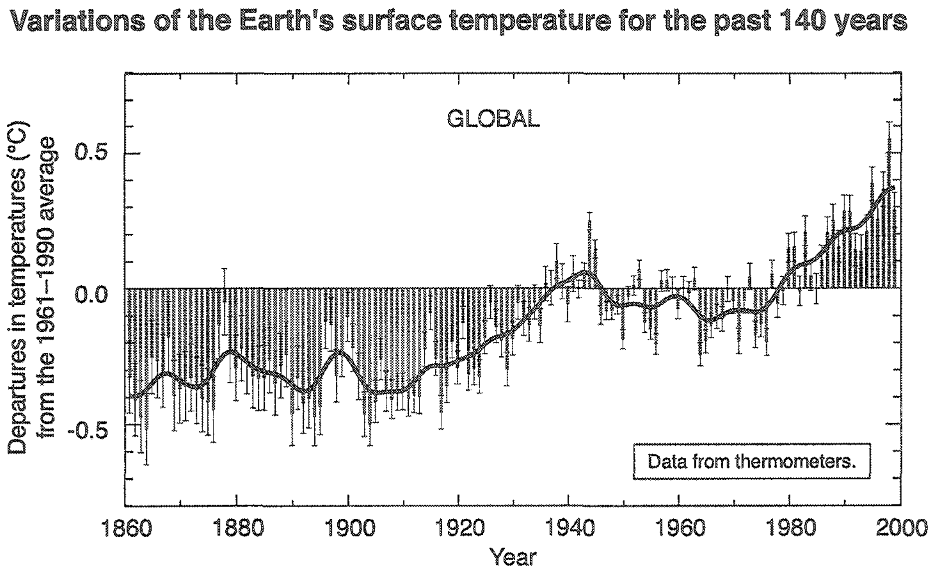

Figure 2: Combined annual land-surface air and sea surface temperature anomalies (°C) 1861 to 1999, relative to 1961 to 1990. Two standard error uncertainties are shown as bars on the annual number. [Based on Figure 2.7c.]

Note: This will be updated in early 2001.

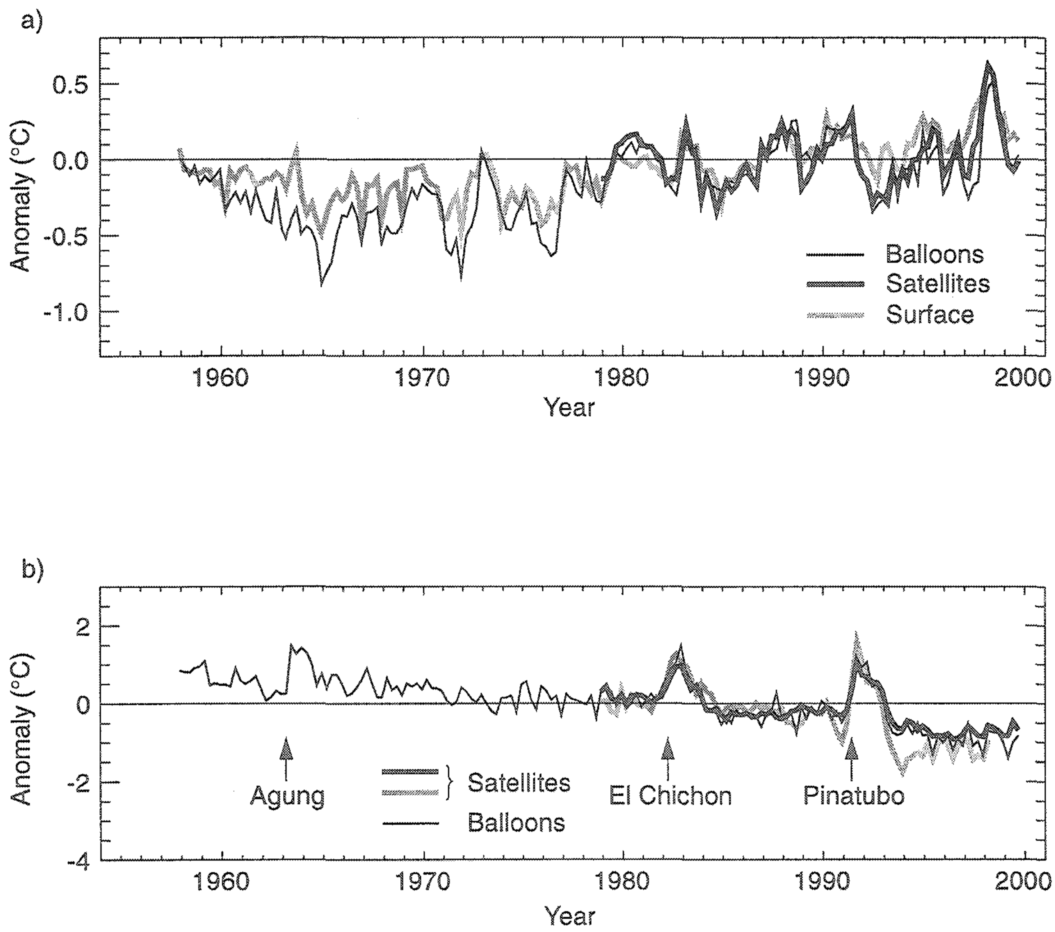

Figure 4: (a) Times series of seasonal temperature anomalies of the troposphere based on balloons and satellites in addition to the surface. (b) Time series of seasonal temperature anomalies of the lower stratosphere from balloons and satellites. [Based on Figure 2.12.]

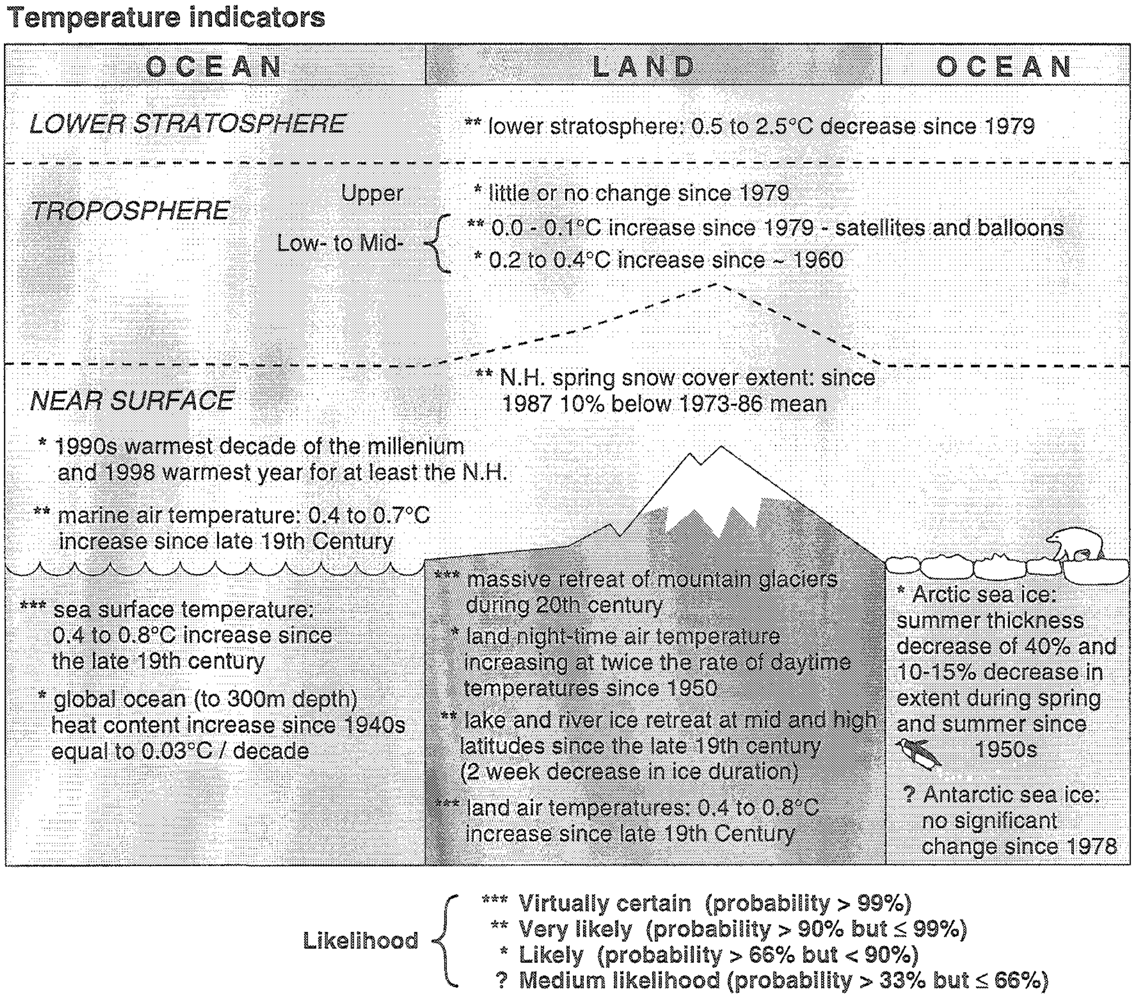

Figure 7a: Schematic of observed variations of the temperature indicators. [Based on Figure 2.39a.]

Hydrological and storm related indicators

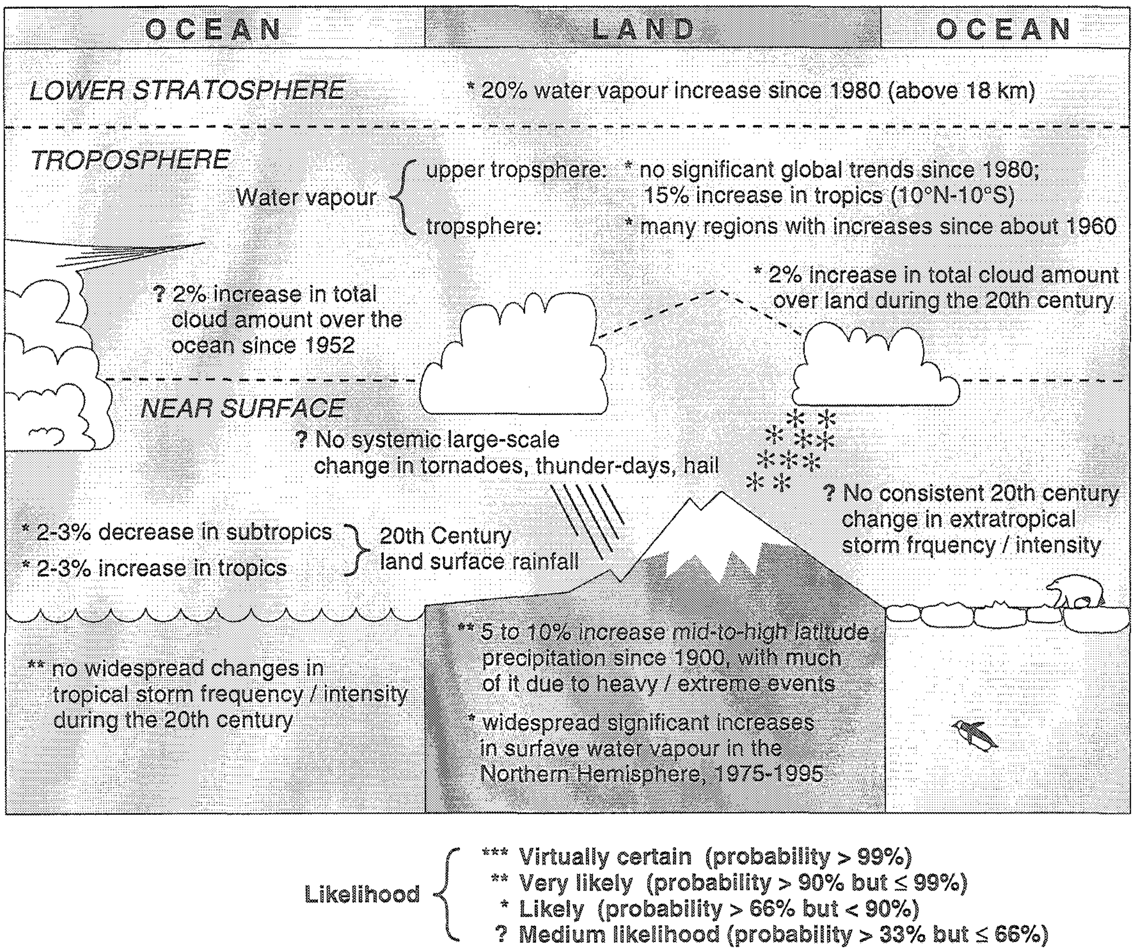

Figure 7b: Schematic of observed variations of the hydrological and storm-related indicators. [Based on Figure 2.39b.]

3. Observed climate change

At the global scale

- The global average surface temperature has increased of 0.6°+/-0.2°C over the 20th century. The last years are likely the warmest of the millennium. The rate of increase is likely unprecedented over the last 10000 years.

- Since the late 1950s the overall global temperature increases in the lowest 8 km of the atmosphere and in surface have been similar at 0.1°C per decade. Over shorter periods, part of the differences of trends at the surface and in the lower atmosphere remain unresolved.

- The warming is confirmed by indirect indicators like mountain glaciers retreat at mid and low latitudes, decrease of snow cover since the late 1960s, Arctic sea-ice extent and thickness decreases during the last decades.

- It is very likely that precipitation has increased in the last century over most mid and high latitudes. Is likely that rainfall has decreased over much of the Northern Hemisphere sub-tropical land areas.

- Changes in tropical and extra-tropical storm intensity and frequency are dominated by inter-decadal to multi-decadal variations.

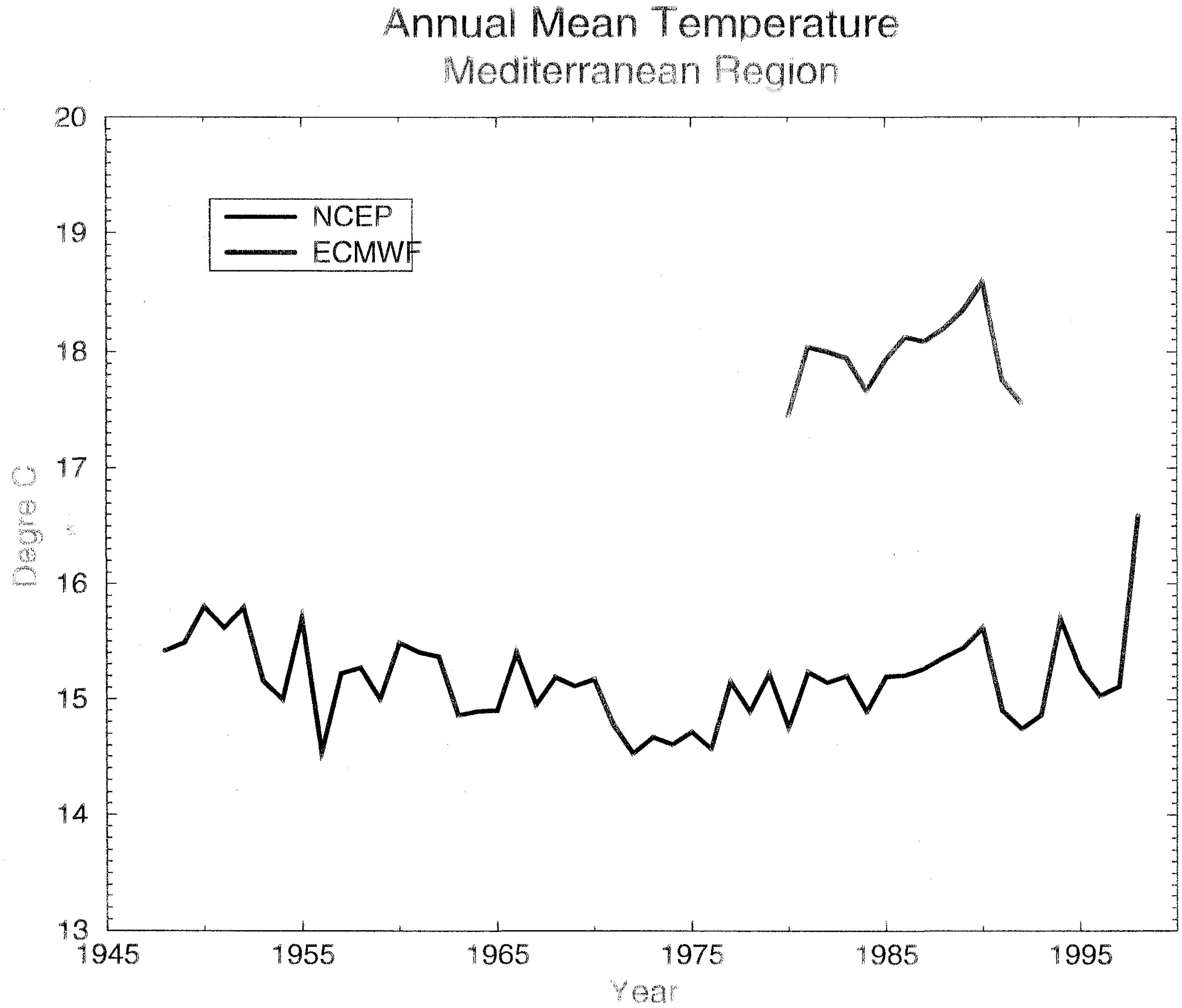
Annual Mean Temperature
Mediterranean Region
NCEP
ECMWF
Degre C
Year
13
14
15
16
17
18
19
20
1945
1955
1965
1975
1985
1995

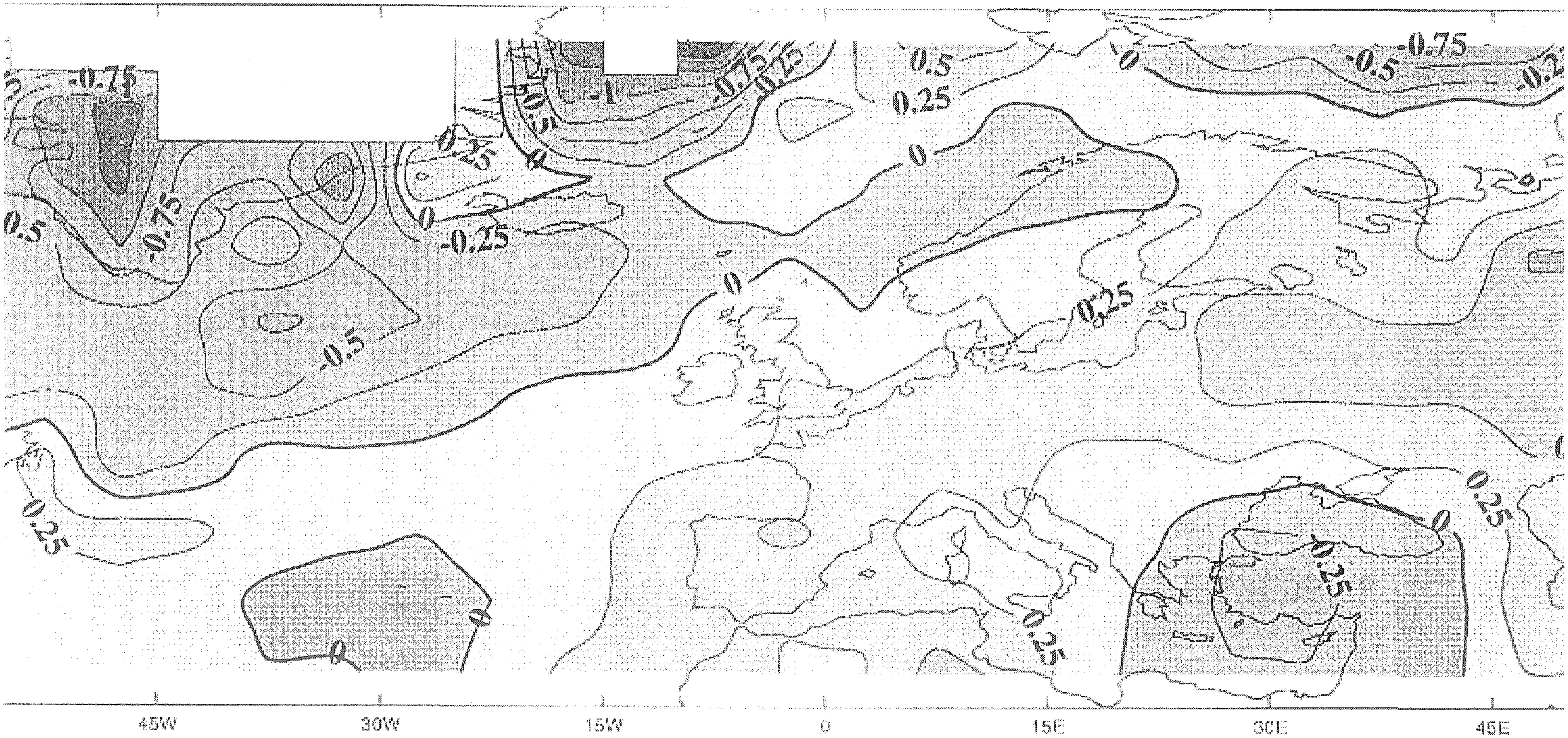

Surface temperature (°C): mean 1931-1990 - mean 1951-1980

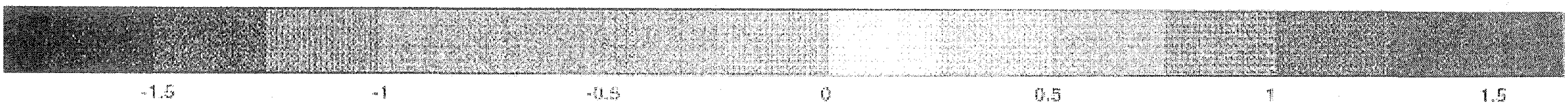

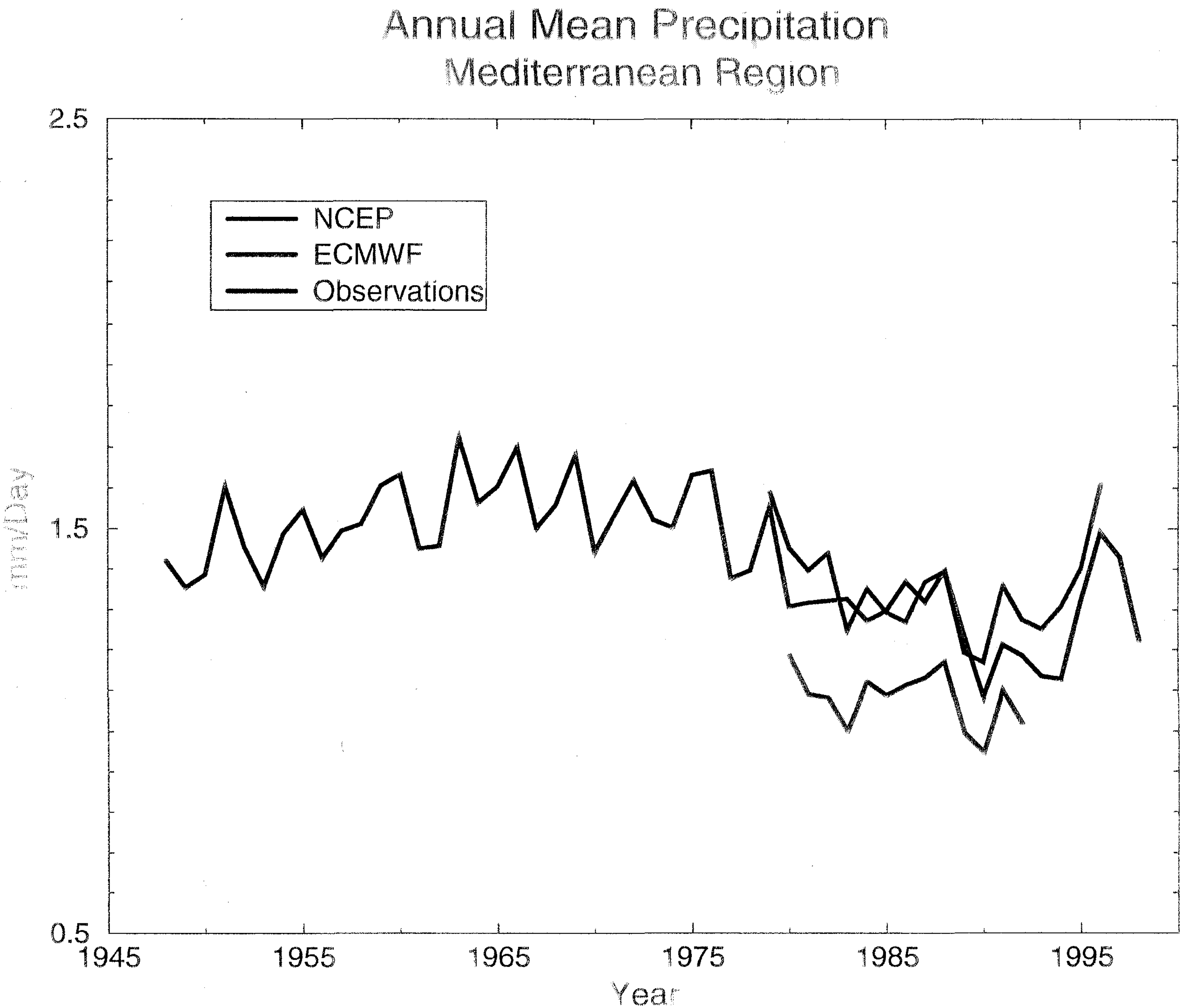
Annual Mean Precipitation
Mediterranean Region
NCEP
ECMWF
Observations
2.5
1.5
0.5
mm/Day
1945
1955
1965
1975
1985
1995
Year

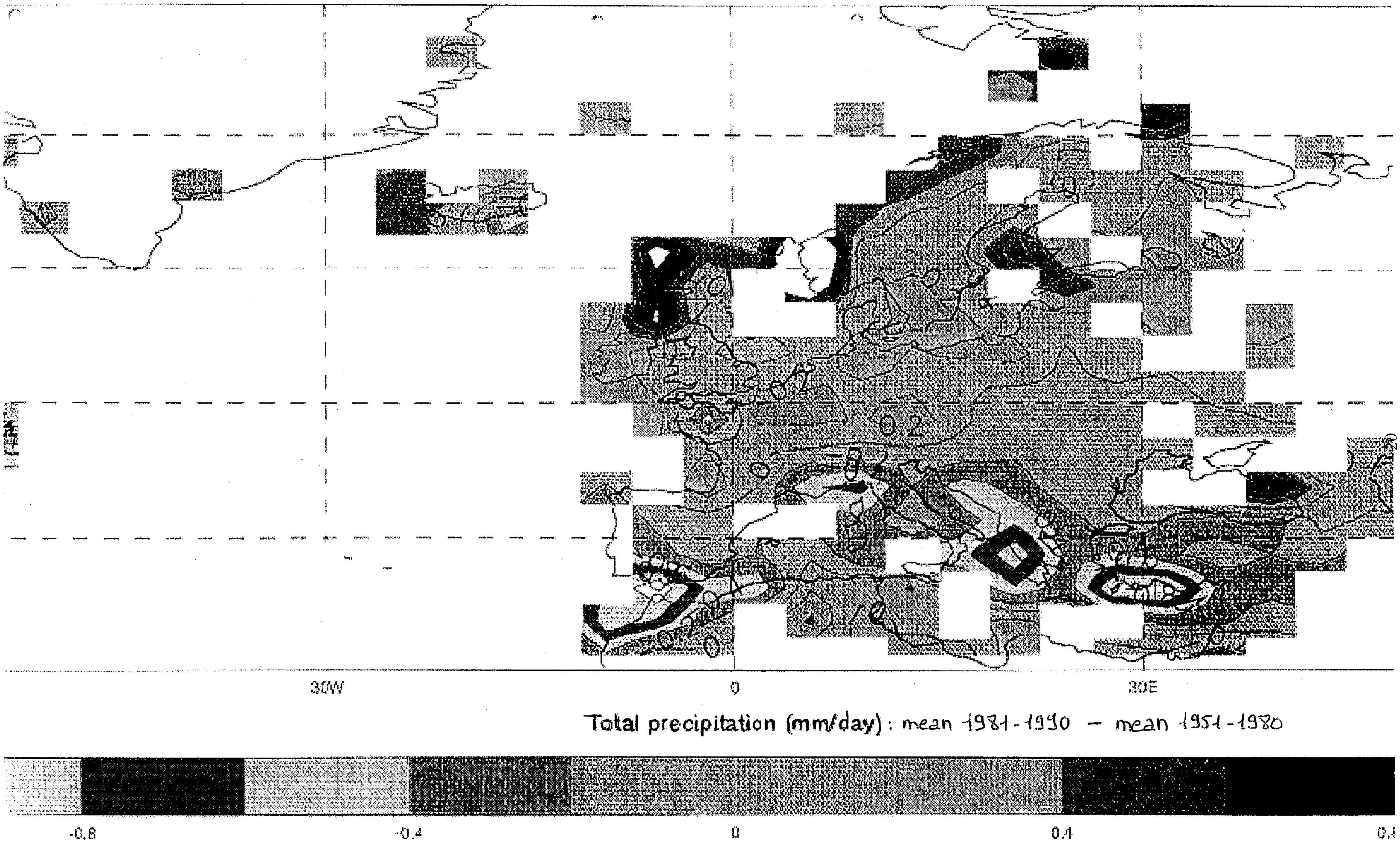

Total precipitation (mm/day) : mean 1981-1990 – mean 1951-1980

3. Observed climate change

Over the Mediterranean area

- The average near surface temperature over the Mediterranean region follows the global average surface temperature at the decadal to multi-decadal time scales. Interannual variability may be marginally influenced by volcanic eruptions.

- The temperature differences between 1981 - 1990 and 1951 - 1980 show a warming of the western part of the Mediterranean basin and a cooling of the eastern part. The warming is greater in summer and in autumn while the cooling is greater in autumn and in winter.

- Average precipitation over the region exhibits no clear tendency over the last decades. Interannual variability is moderate but may be very significant at some locations.

- Precipitation differences between 1981 - 1990 and 1951 - 1980 show a decrease over the basin excepted in Tunisia and over northern Algeria (but ECSN data coverage is limited to 32°N). Local long series from south of Spain show that recent drought conditions are similar to other ones observed at the end of 19th century.

- As for many other regions, climate datasets exist for the Mediterranean area, however they are often on paper support and need quality control with the application of homogenisation processes.

4. Projected climate change

The models and the simulations

- A hierarchy from simple energy budget models to complex coupled GCMs and regional models.

  Energy budget and upwelling/diffusion simple models to assess changes in global average temperature. The parameters of these models, like climate sensitivity, must be adjusted on the results of General Circulation Models.

  Atmospheric General Circulation models simulating equilibrium climate under present conditions and under doubled CO2 conditions, to investigate the role of some processes on climate change or improve the resolution of the simulations.

  Coupled atmospheric and oceanic GCMs to simulate transitory climate change over decades or centuries. These models more and more include the coupling to other components of the climate system (sea-ice, ice-cap, chemistry, ecosystems, hydrology, biology, ...).

  Regional area limited atmospheric models of variable resolution atmospheric GCMs to simulate regional features of climate change (dynamical downscalling). Coupling with other components has been recently developed.

4. Projected climate change

The models and the simulations

- Models must be validated on present climate or past climate conditions using natural and anthropogenic forcings.

- Construction of climate scenarios for impact, adaptation and mitigation through the simulation of climate in response to scenarios of greenhouse gases and aerosols concentrations. These scenarios come from emission scenarios like those of the IPCC Special Report on Emission Scenarios (SRES).

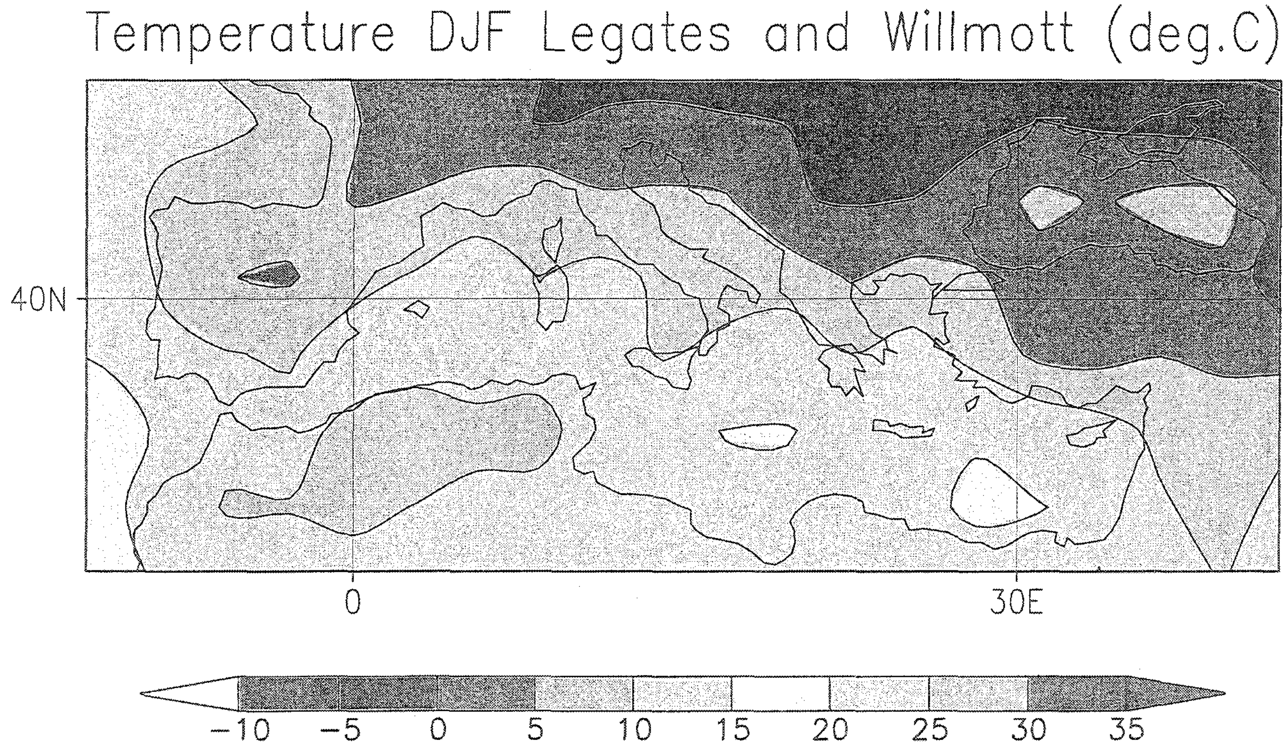
Temperature DJF Legates and Willmott (deg.C)
40N
0
30E
−10 −5 0 5 10 15 20 25 30 35

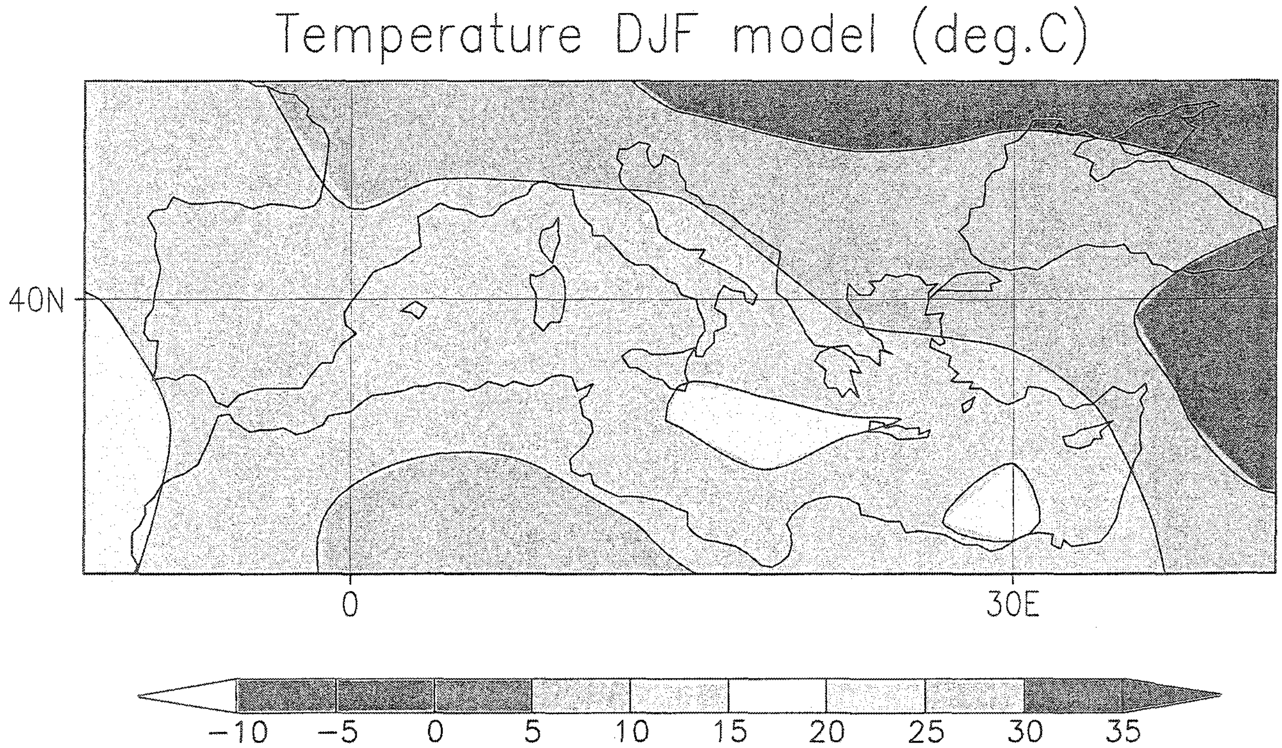
Temperature DJF model (deg.C)
40N
0
30E
−10 −5 0 5 10 15 20 25 30 35

Temperature JJA Legates and Willmott (deg.C)

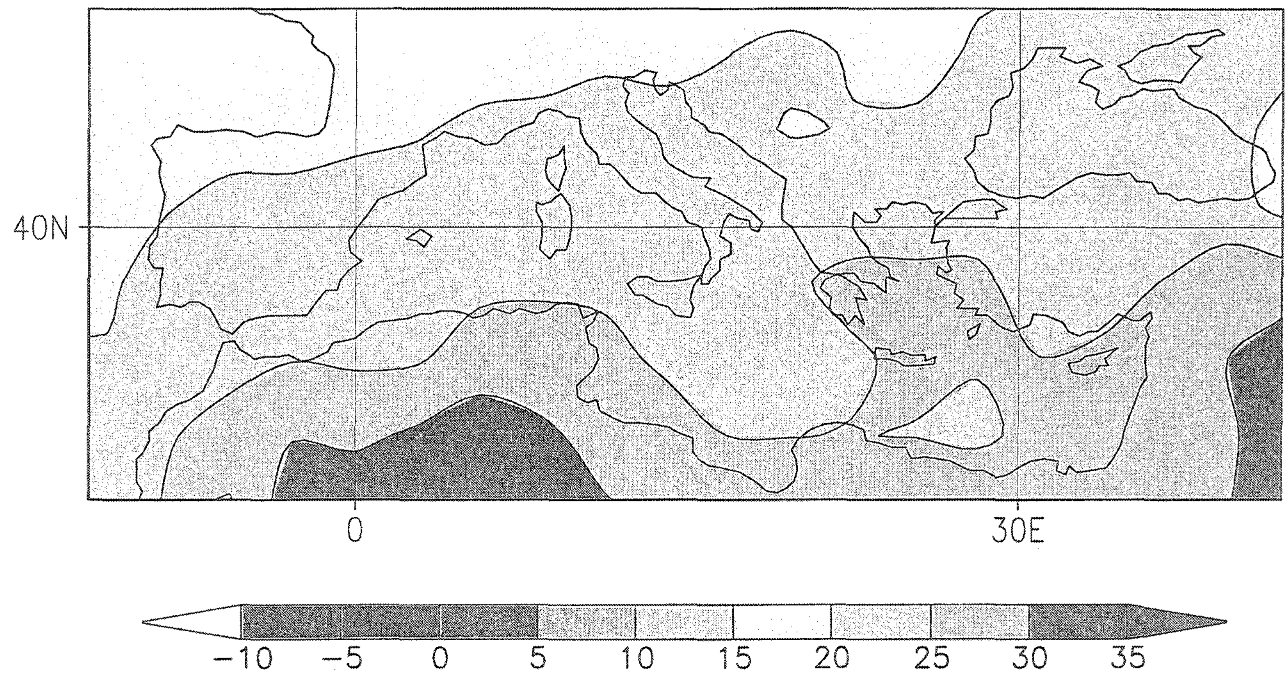

Temperature JJA model (deg.C)

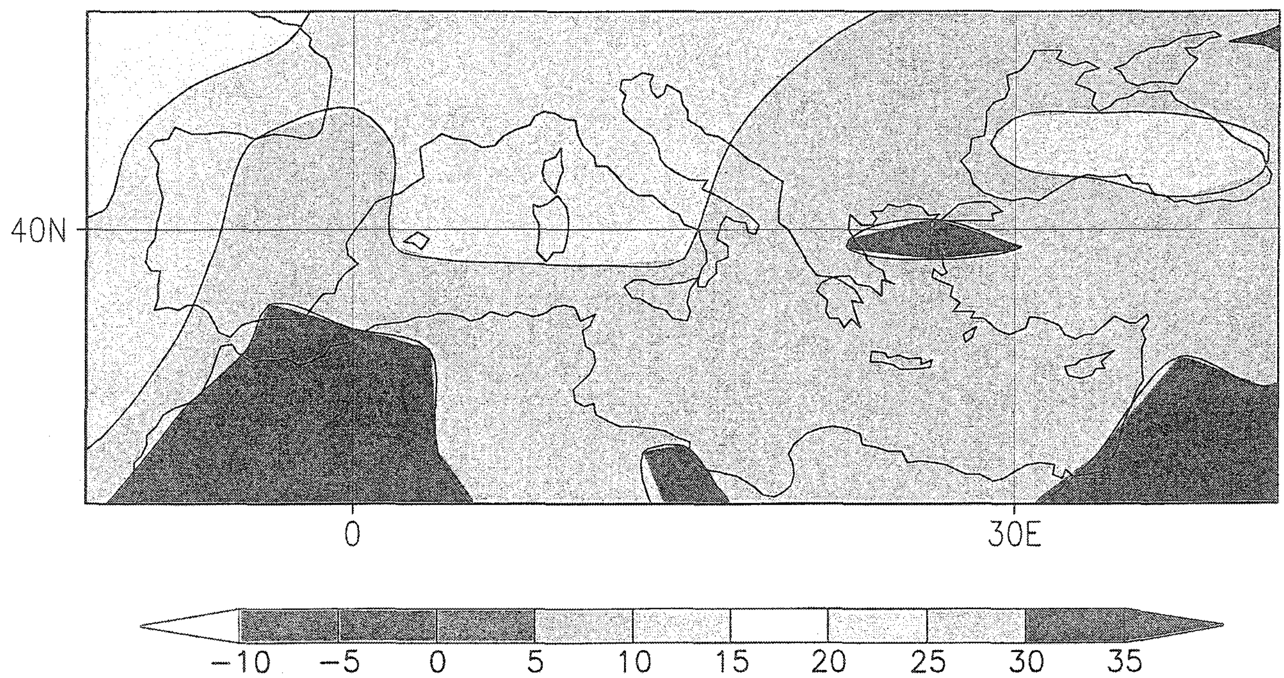

Precipitations DJF Xie and Arkin (mm/day)

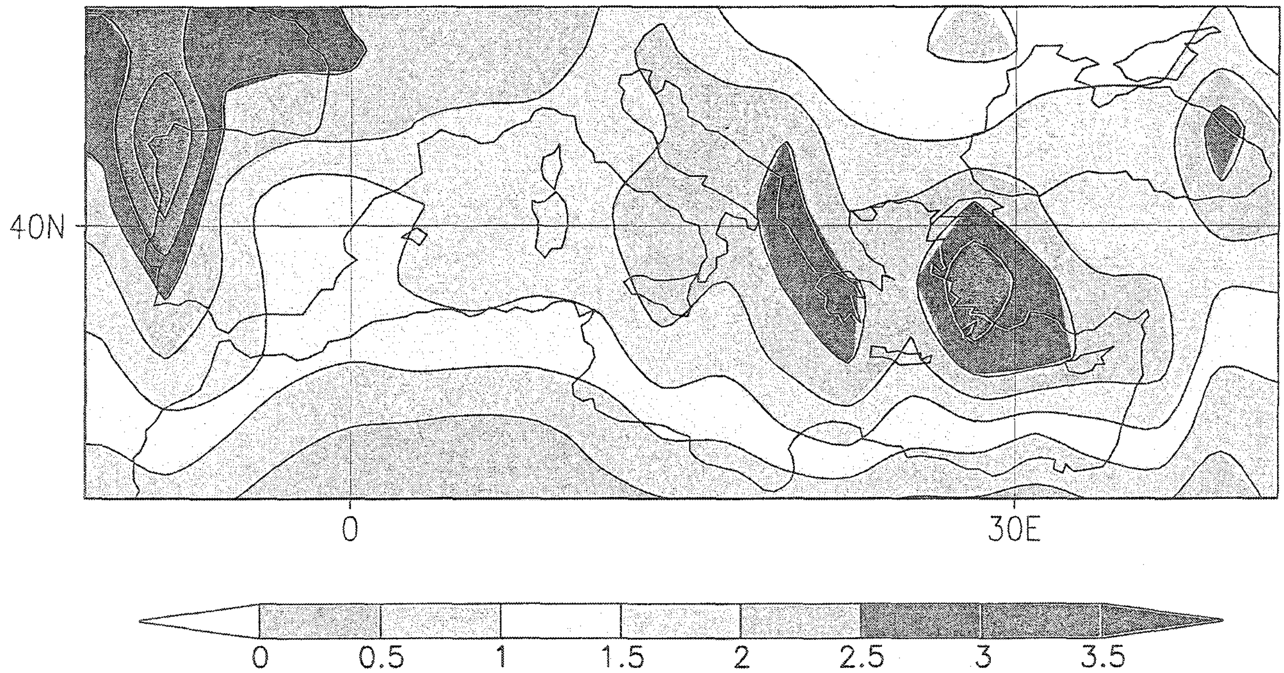

Precipitations DJF model (mm/day)

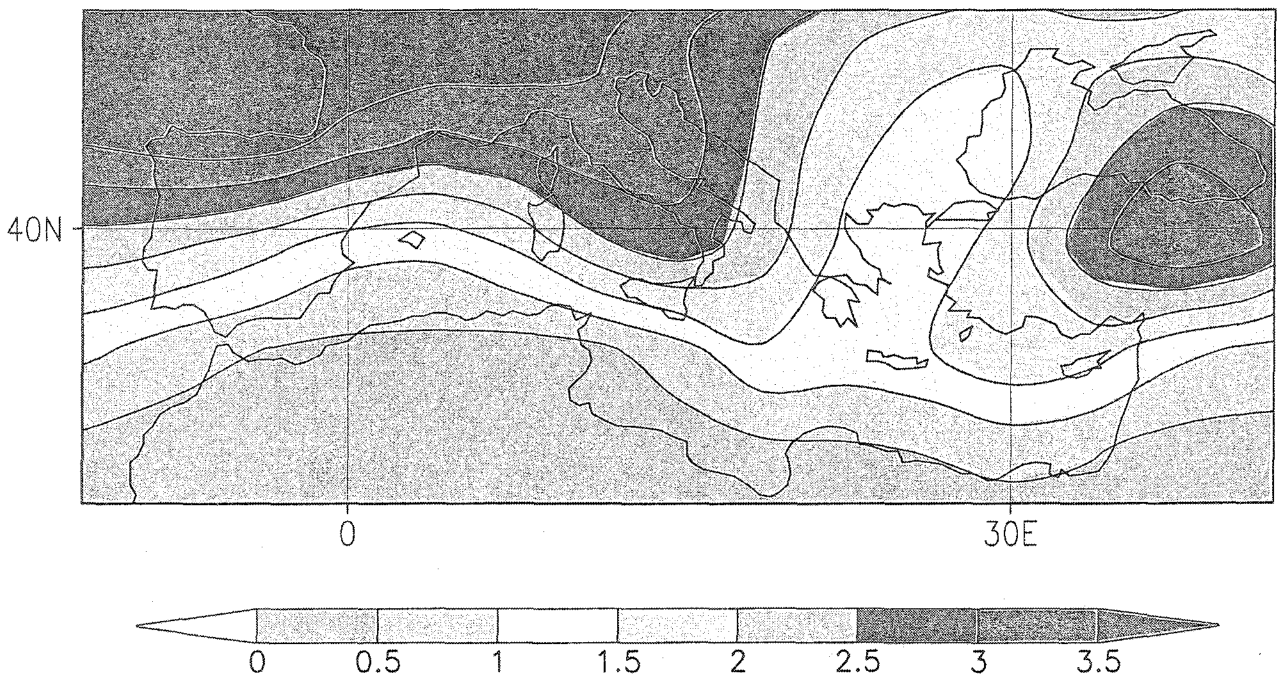

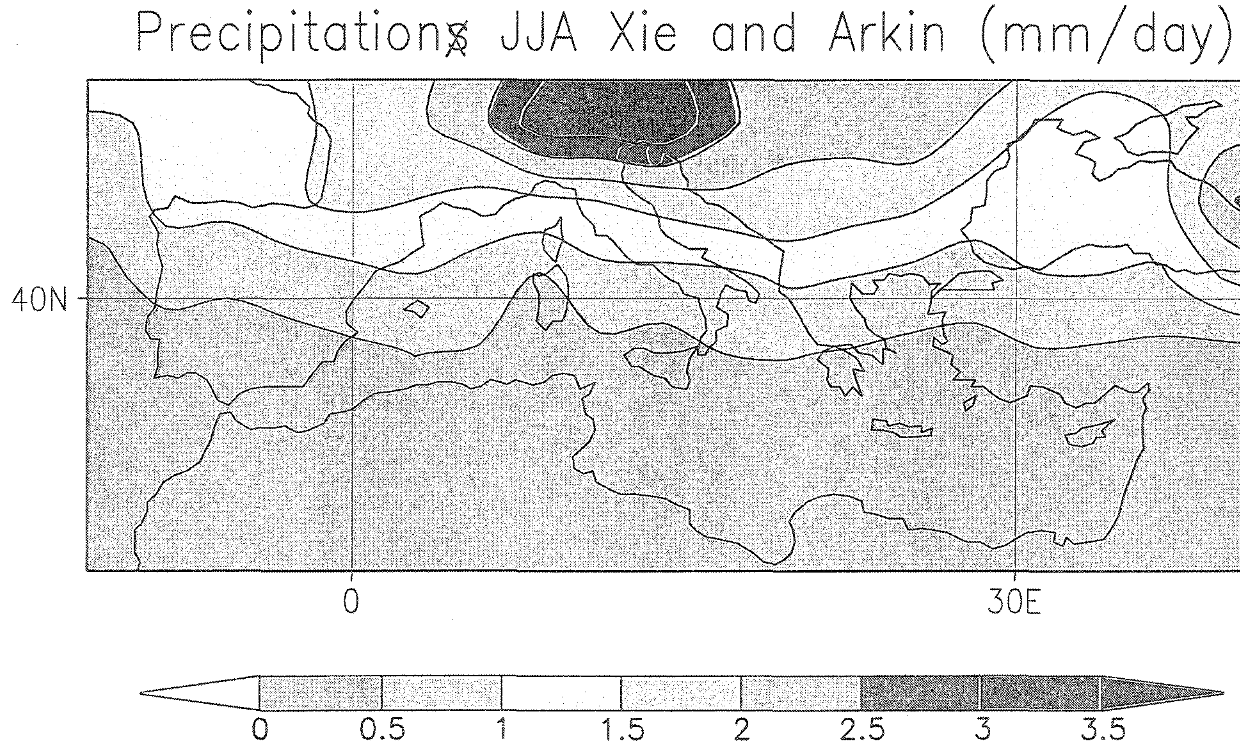
Precipitation JJA Xie and Arkin (mm/day)
40N
0
30E
0
0.5
1
1.5
2
2.5
3
3.5

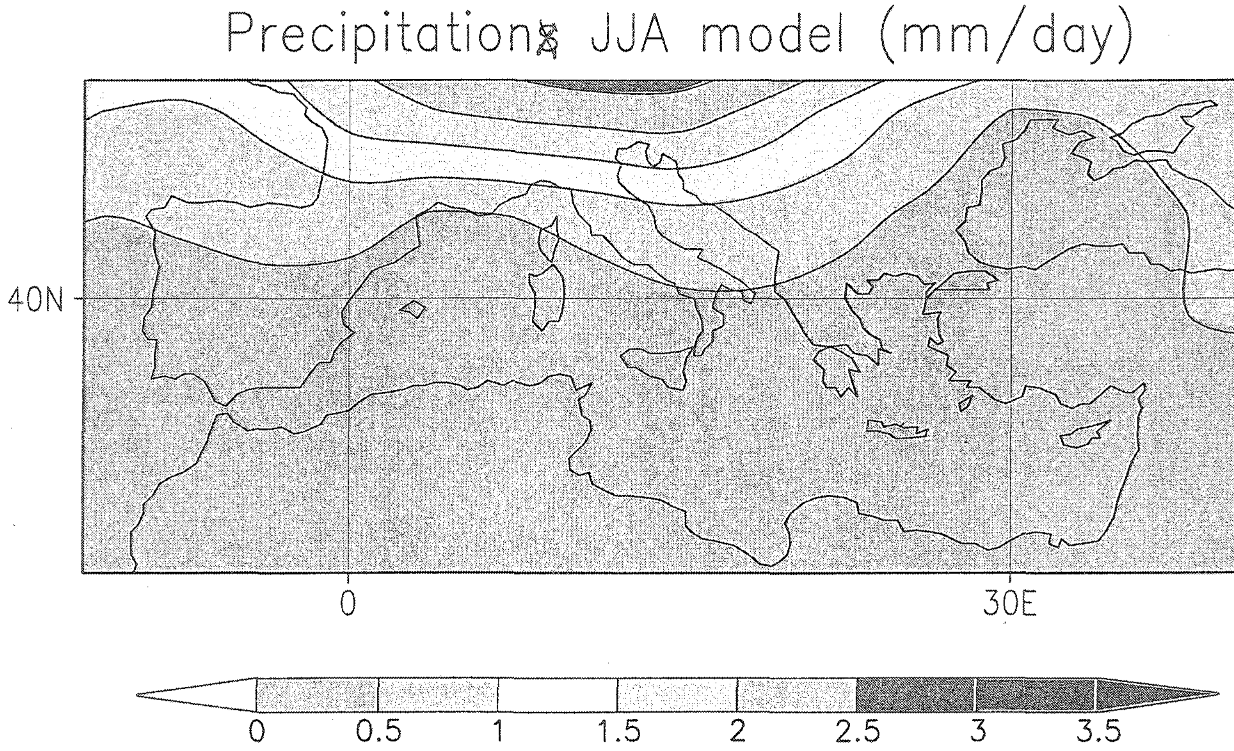
Precipitation JJA model (mm/day)
40N
0
30E
0
0.5
1
1.5
2
2.5
3
3.5

Biaises for 1961-1990 for simulations with historical forcing including sulphate aerosols

Temperature	
Winter	-0.7°C / +3.0°C
Summer	-1.0°C / +5.1°C

Precipitation	
Winter	-20% / +15%
Summer	-31% / +15%

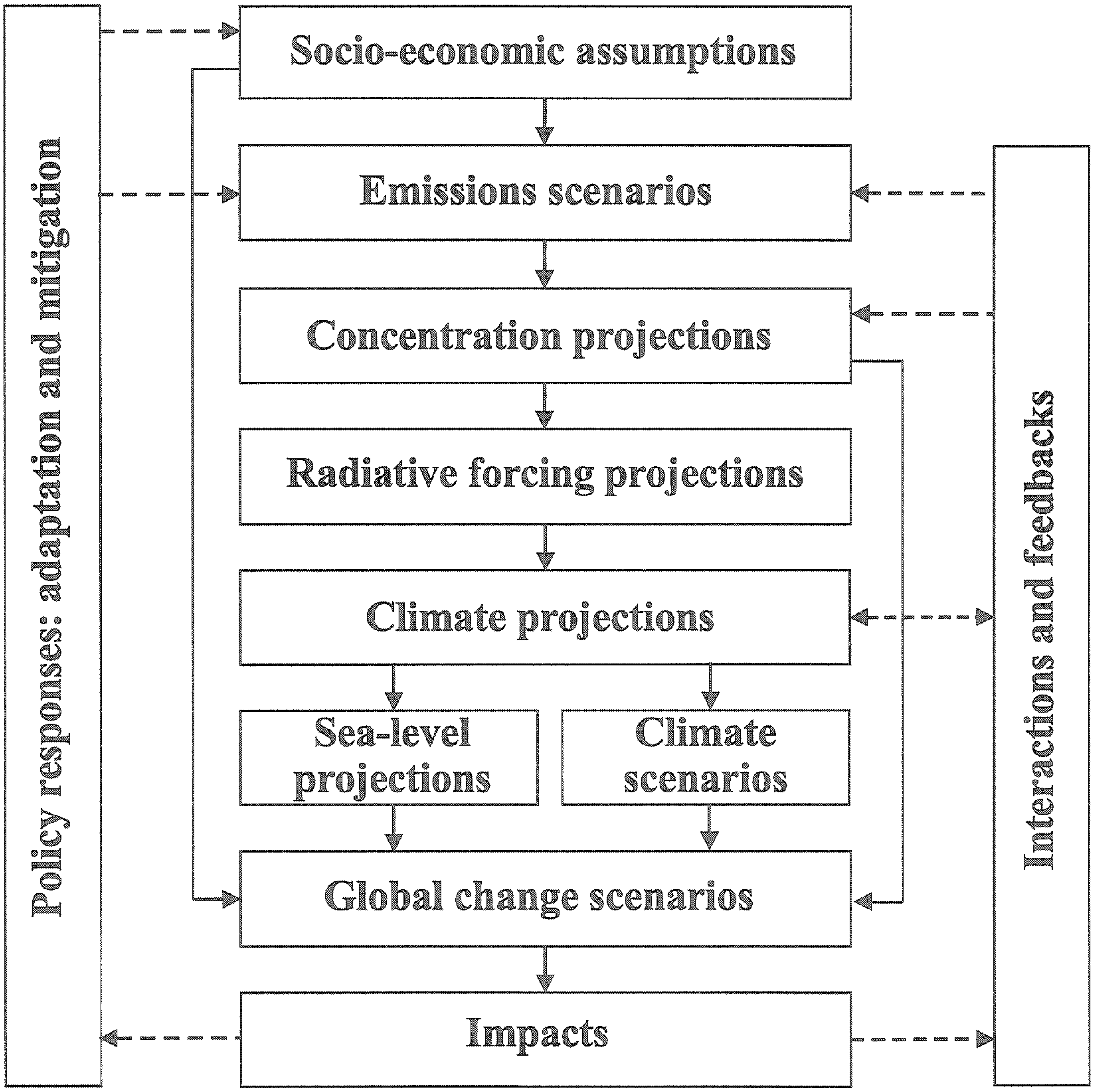

Figure 27: The cascade of uncertainties in projections to be considered in developing climate and related scenarios for climate change impact, adaptation, and mitigation assessment. [Based on Figure 13.2.]

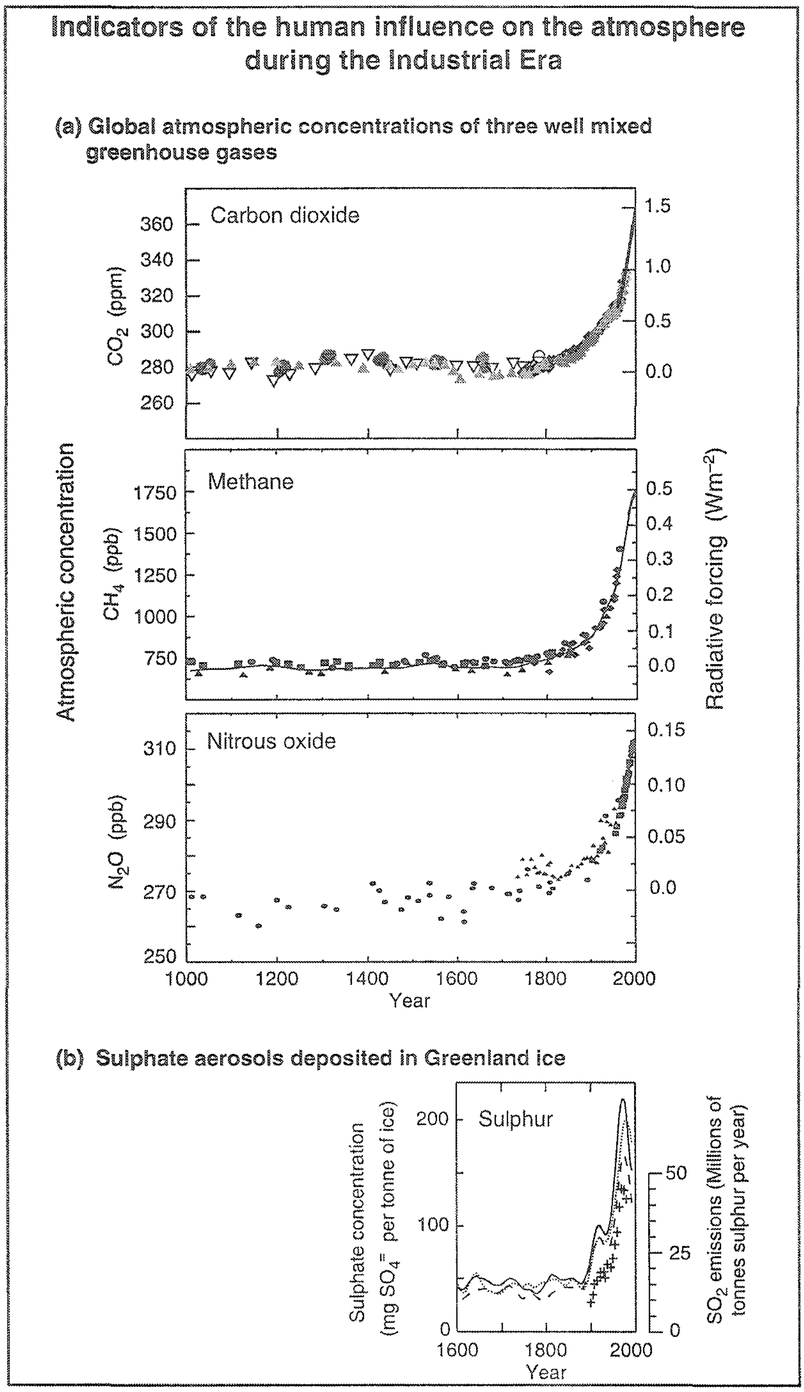

Figure 2: Long records of past changes in atmospheric composition provide the context for the influence of anthropogenic emissions.

(a) shows changes in the atmospheric concentrations of carbon dioxide (CO_2), methane (CH_4), and nitrous oxide (N_2O) over the past 1000 years. The ice core and firn data for several sites in Antarctica and Greenland (shown by different symbols) are supplemented with the data from direct atmospheric samples over the past few decades (shown by the line for CO_2 and incorporated in the curve representing the global average of CH_4). The estimated positive radiative forcing of the climate system from these gases is indicated on the right-hand scale. Since these gases have atmospheric lifetimes of a decade or more, they are well mixed, and their concentrations reflect emissions from sources throughout the globe. All three records show effects of the large and increasing growth in anthropogenic emissions during the Industrial Era.

(b) illustrates the influence of industrial emissions on atmospheric sulphate concentrations, which produce negative radiative forcing. Shown is the time history of the concentrations of sulphate, not in the atmosphere but in ice cores in Greenland (shown by lines; from which the episodic effects of volcanic eruptions have been removed). Such data indicate the local deposition of sulphate aerosols at the site, reflecting sulphur dioxide (SO_2) emissions at mid-latitudes in the Northern Hemisphere. This record, albeit more regional than that of the globally-mixed greenhouse gases, demonstrates the large growth in anthropogenic SO_2 emissions during the Industrial Era. The pluses denote the relevant regional estimated SO_2 emissions (right-hand scale).

[Based upon (a) Chapter 3, Figure 3.2b (CO_2); Chapter 4, Figure 4.1a and b (CH_4) and Chapter 4, Figure 4.2 (N_2O) and (b) Chapter 5, Figure 5.4a]

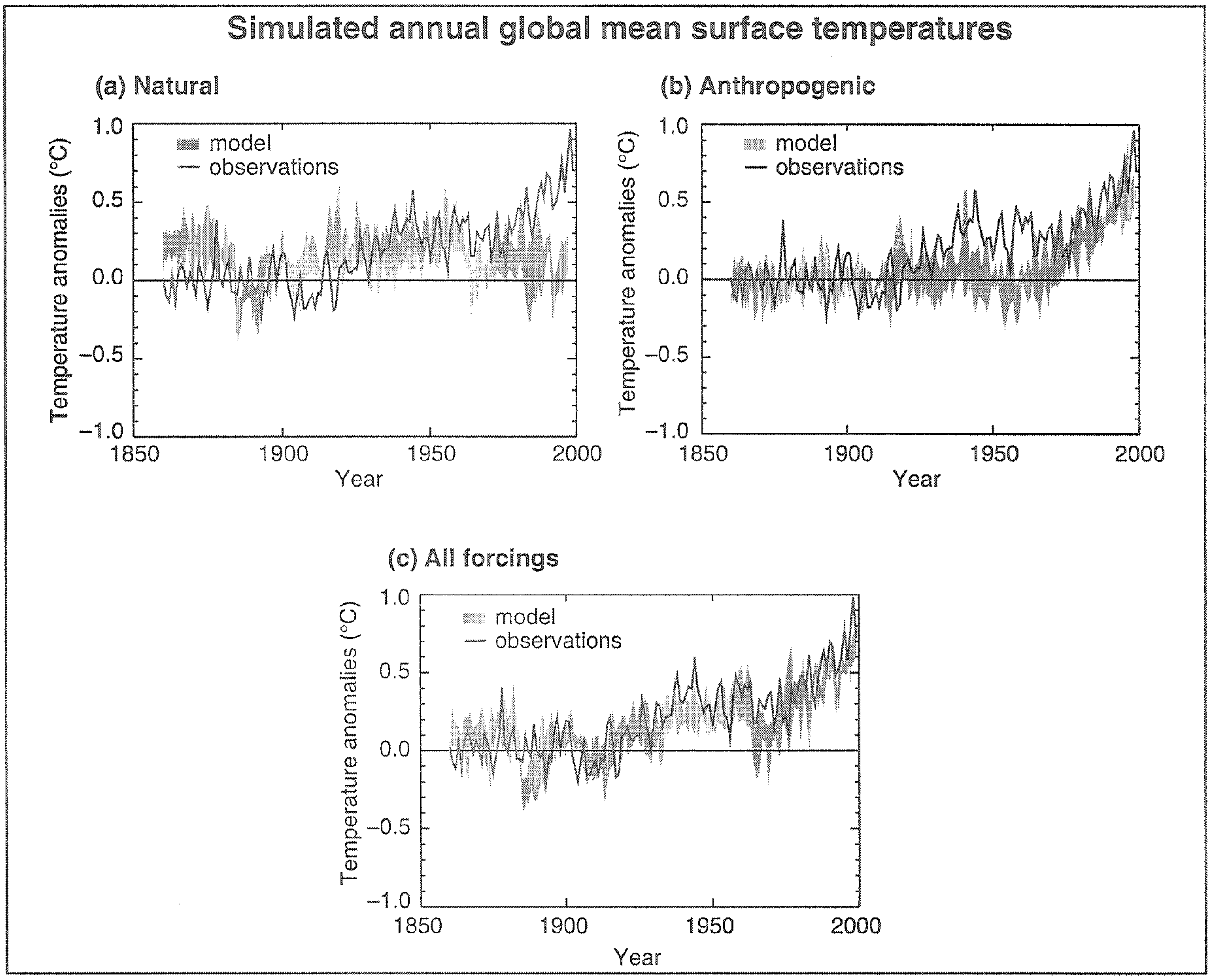

Figure 4: Simulating the Earth's temperature variations, and comparing the results to measured changes, can provide insight into the underlying causes of the major changes.

A climate model can be used to simulate the temperature changes that occur both from natural and anthropogenic causes. The simulations represented by the band in (a) were done with only natural forcings: solar variation and volcanic activity. Those encompassed by the band in (b) were done with anthropogenic forcings: greenhouse gases and an estimate of sulphate aerosols, and those encompassed by the band in (c) were done with both natural and anthropogenic forcings included. From (b), it can be seen that inclusion of anthropogenic forcings provides a plausible explanation for a substantial part of the observed temperature changes over the past century, but the best match with observations is obtained in (c) when both natural and anthropogenic factors are included. These results show that the forcings included are sufficient to explain the observed changes, but do not exclude the possibility that other forcings may also have contributed. The bands of model results presented here are for four runs from the same model. Similar results to those in (b) are obtained with other models with anthropogenic forcing. [Based upon Chapter 12, Figure 12.7]

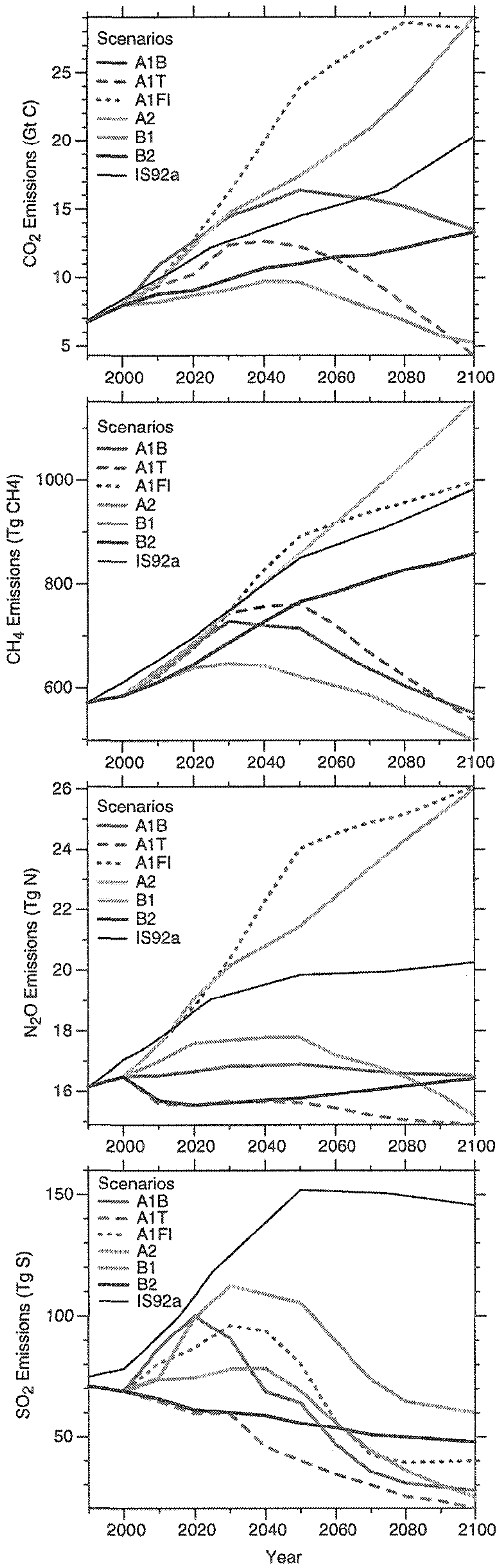

Figure 16: Anthropogenic emissions of CO_2, CH_4, N_2O and sulphur dioxide for the six illustrative SRES scenarios, A1B, A2, B1 and B2, A1FI and A1T. For comparison the IS92a scenario is also shown. [Based on IPCC Special Report on Emissions Scenarios.]

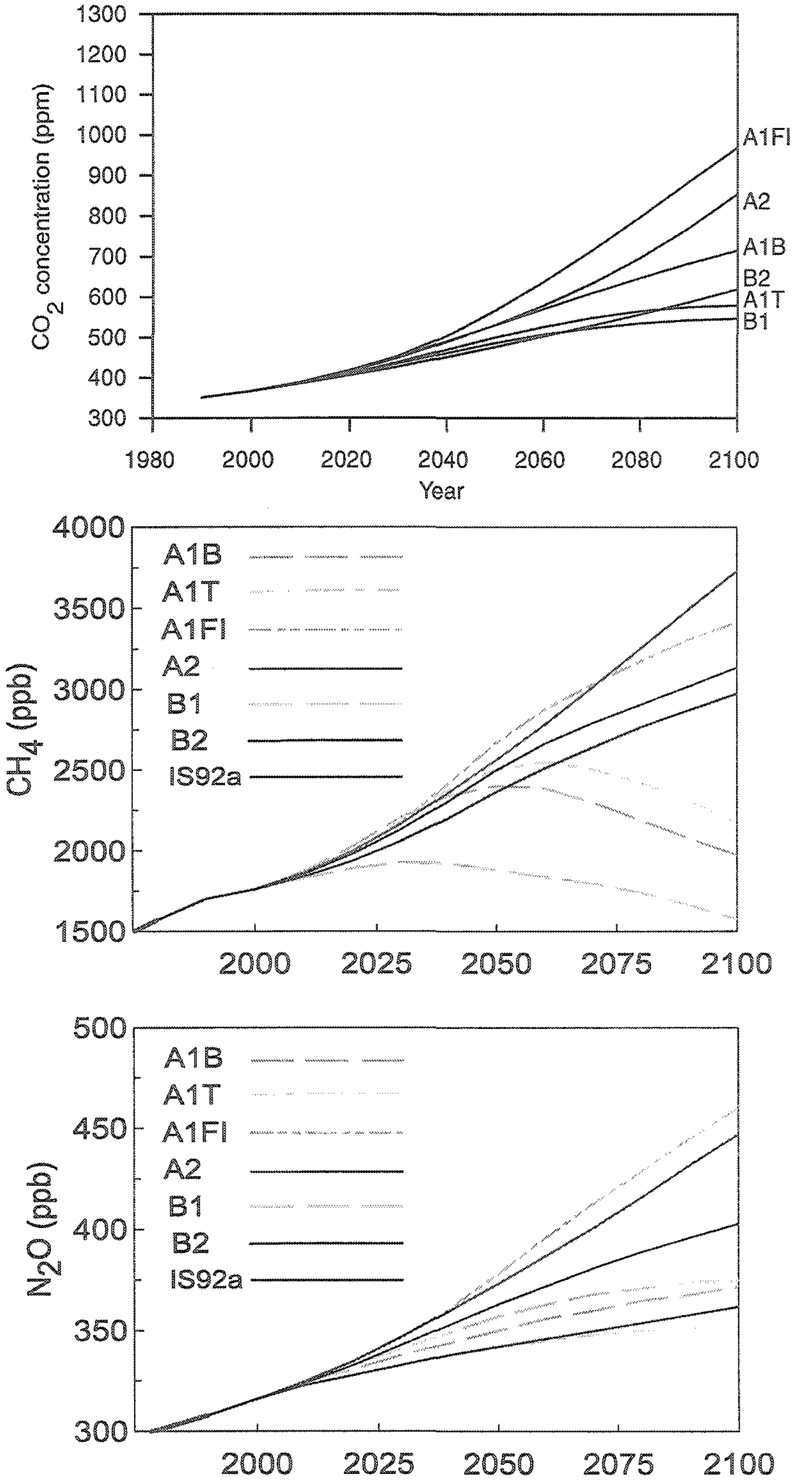

Figure 17: Atmospheric concentrations of CO_2, CH_4 and N_2O resulting from the six SRES scenarios and from the IS92a scenario computed with current methodology. [Based on Figures 3.12 and 3.14a-1 and 2.]

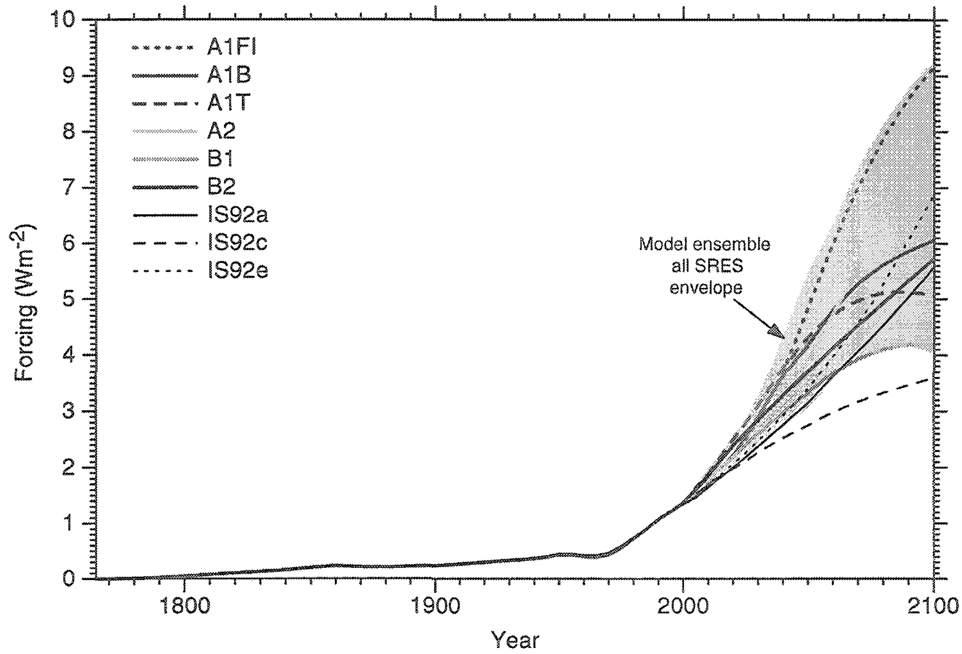

Figure 18: Simple model results: estimated historical anthropogenic radiative forcing up to 2000 followed by radiative forcing for the six illustrative SRES scenarios. The shading shows the envelope of forcing that encompasses the full set of thirty-five SRES scenarios. The method of calculation closely follows that explained in the chapters. The values are based on the radiative forcing for a doubling of CO_2 from seven AOGCMs. The IS92a, IS92c, and IS92e forcing is also shown following the same method of calculation. [Based on Figure 9.13a.]

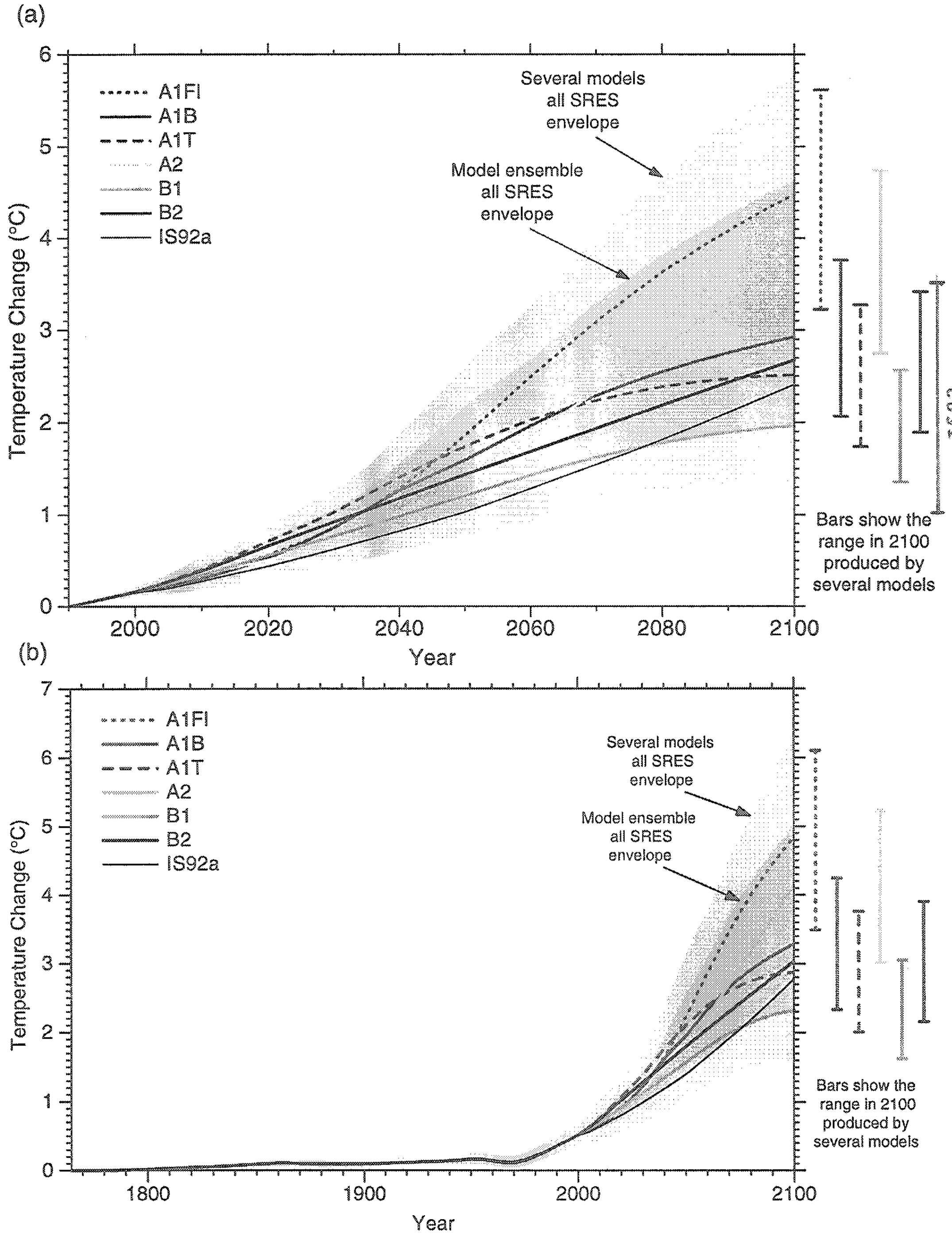

Figure 21: Simple model results: (a) global mean temperature projections for the six illustrative SRES scenarios using a simple climate model tuned to seven AOGCMs. Also for comparison, following the same method, results are shown for IS92a. The darker shading represents the envelope of the full set of thirty-five SRES scenarios using the average of the model results (mean climate sensitivity is 2.8°C). The lighter shading is the envelope based on all seven model projections (with climate sensitivity in the range 1.7 to 4.2°C). The bars show, for each of the six illustrative SRES scenarios, the range of simple model results in 2100 for the seven AOGCM model tunings. (b) Same as (a) but results include estimated historical anthropogenic forcing. [Based on Figures 9.14 and 9.13b.]

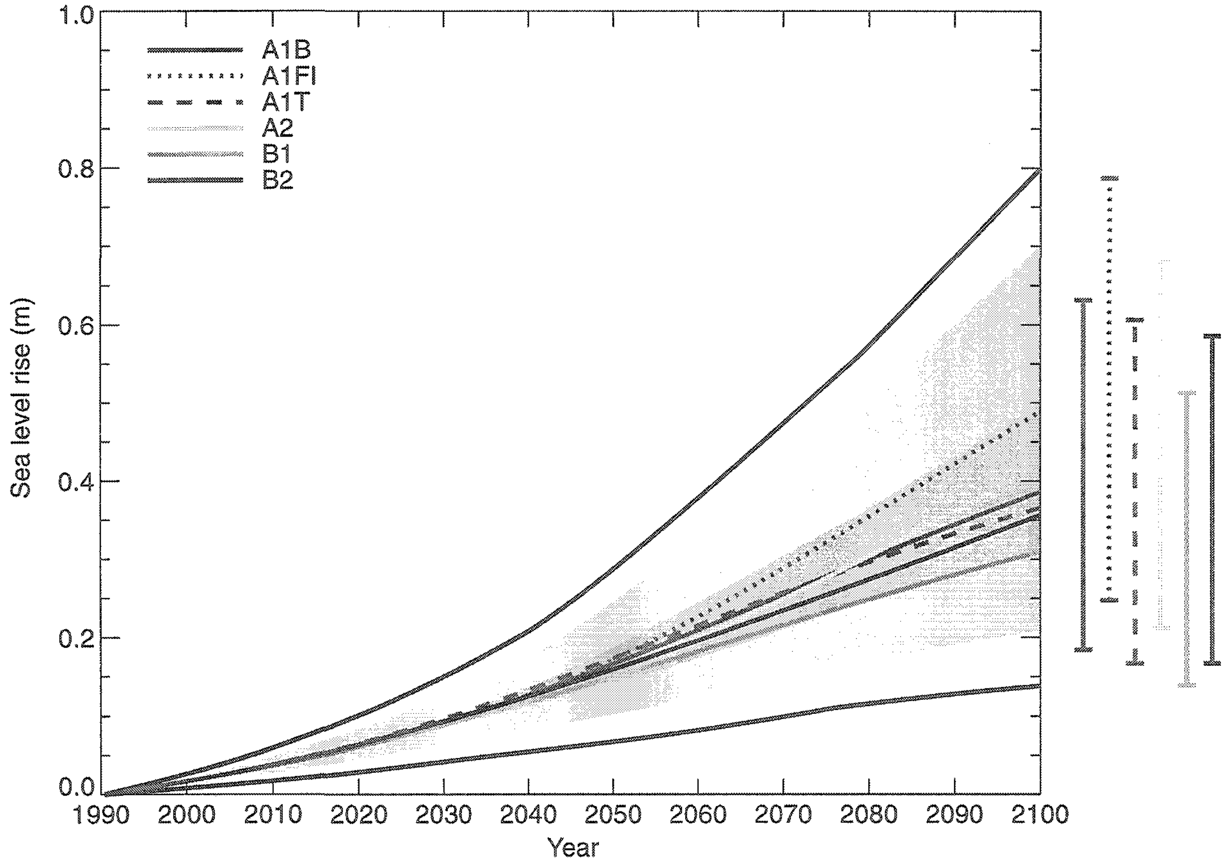

Figure 23: Global-average sea-level rise 1990-2100 for the SRES scenarios. Thermal expansion and land ice changes were calculated using a simple climate model calibrated separately for each of seven AOGCMs, and contributions from changes in permafrost, the effect of sediment deposition and the long-term adjustment of the ice-sheets to past climate change were added. Each of the six lines appearing in the key is the average of AOGCMs for one of the six illustrative scenarios. The region in dark shading shows the range of the average of AOGCMs for all 35 SRES scenarios. The region in light shading shows the range of all AOGCMs for all 35 scenarios. The region delimited by the outermost lines shows the range of all AOGCMs and scenarios including uncertainty in land-ice changes, permafrost changes and sediment deposition. [Based on Figure 11.12.]

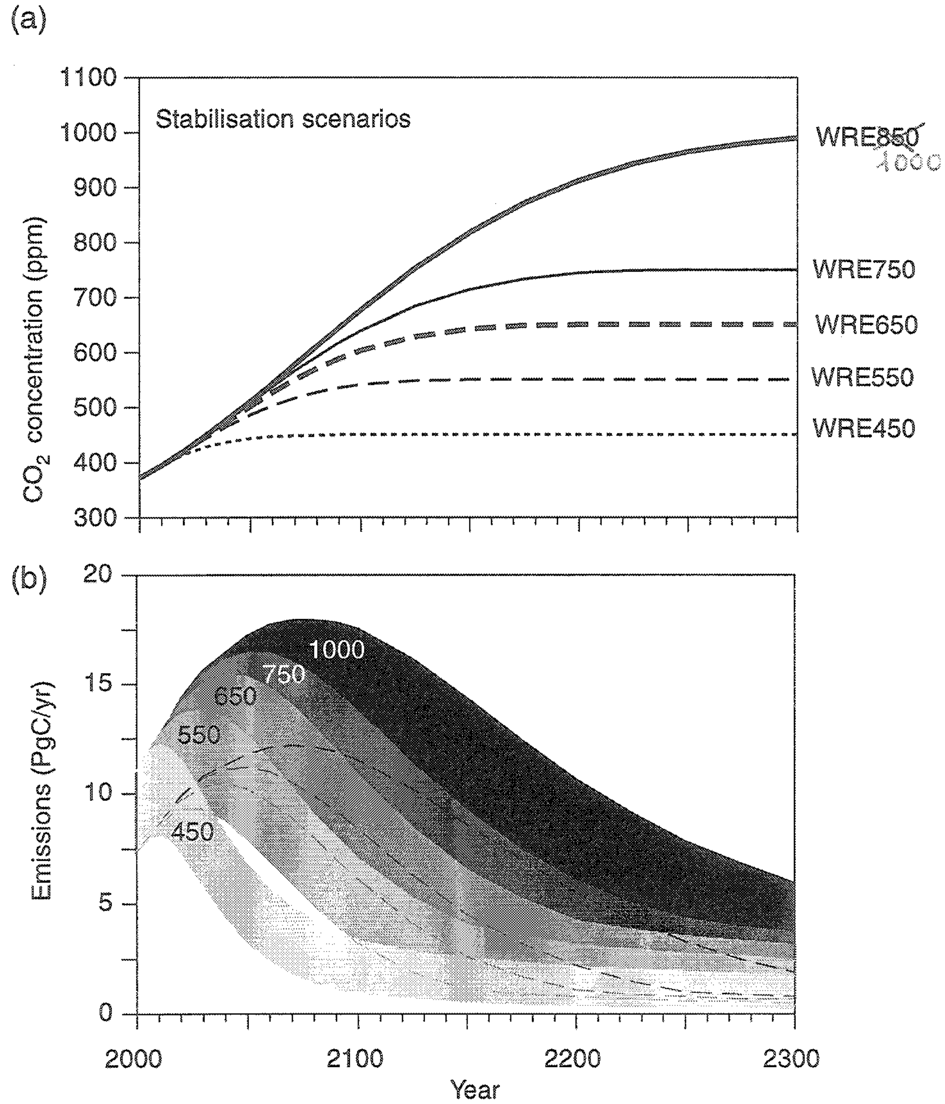

Figure 24: Projcted CO_2 emissions permitting stabilization of atmospheric CO_2 concentrations at different final values. Panel (a) shows the assumed trajectories of CO_2 concentration (WRE scenarios) and panels (b) and (c) show the implied CO_2 emissions, as projected with two fast carbon cycle models, Bern-CC and ISAM. The model ranges for ISAM were obtained by tuning the model to approximate the range of responses to CO_2 and climate from model intercomparisons. This approach yields a lower bound on uncertainties in the carbon cycle response. The model ranges for Bern-CC were obtained by combining different bounding assumptions about the behaviour of the CO_2 fertilization effect, the response of heterotrophic respiration to temperature and the turnover time of the ocean, thus approaching an upper bound on uncertainties in the carbon cycle response. For each model, the upper and lower bounds are indicated by the top and bottom of the shaded area. Alternatively, the lower bound (where hidden) is indicated by a hatched line. [Based on Figure 11.12.]

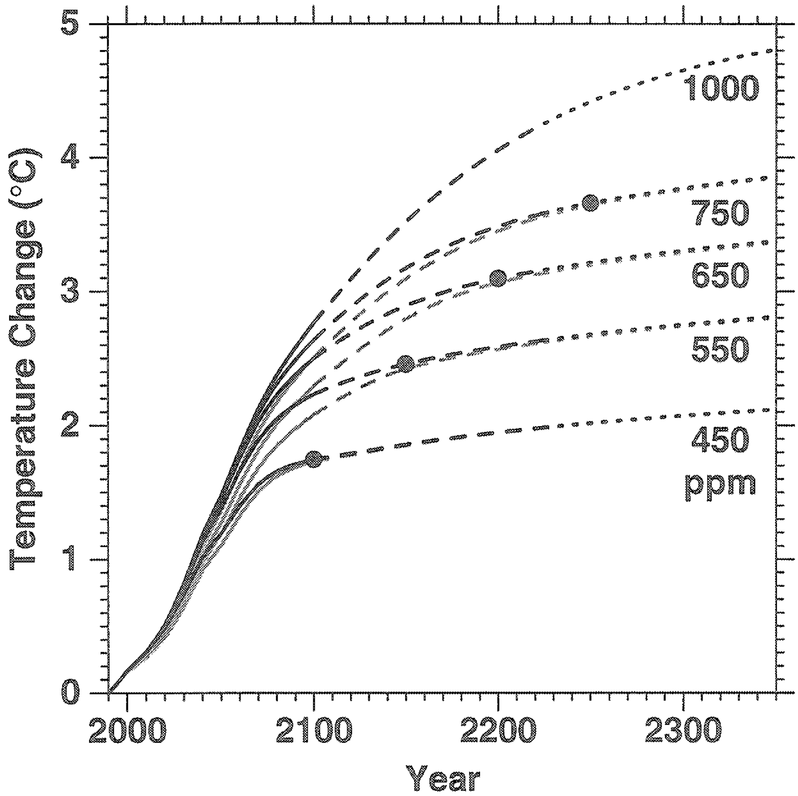

Figure 25: Simple model results: Projected global mean temperature changes when the concentration of CO_2 is stabilised following the WRE profiles (see chapter 9.3.3). For comparison, results based on the S profiles in the SAR are also shown in blue (S1000 not available). The results are the average produced by a simple climate model tuned to seven AOGCMs. The baseline scenario is scenario A1B, this is specified only to 2100. After 2100, the emissions of gases other than CO_2 are assumed to remain constant at their A1B 2100 values. The projections are labelled according to the level of CO_2 stabilisation. The broken lines after 2100 indicate increased uncertainty in the simple climate model results beyond 2100. The black dots indicate the time of CO_2 stabilisation. The stabilisation year for the WRE1000 profile is 2375. [Based on Figure 9.16.]

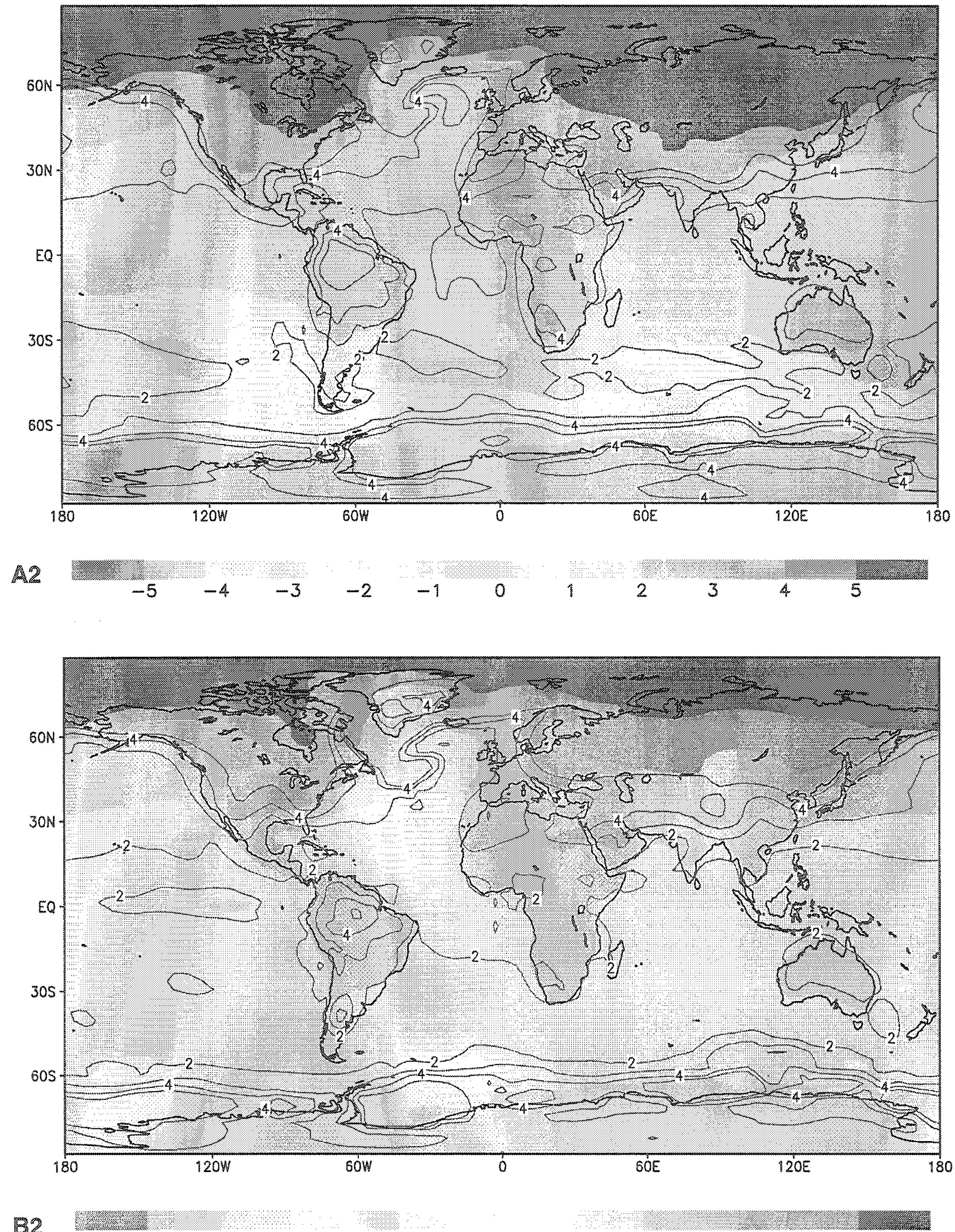

Figure 19: The annual mean change of the temperature (colour shading) and its range (isolines) [Unit: °C] for the SRES scenario A2 (upper panel) and the SRES scenario B2 (lower panel). Both SRES-scenarios show the period 2071-2100 relative to the period 1961-1990 and where performed by OAGCMs. [Based on Figures 9.10d-1 and 9.10e-1.]

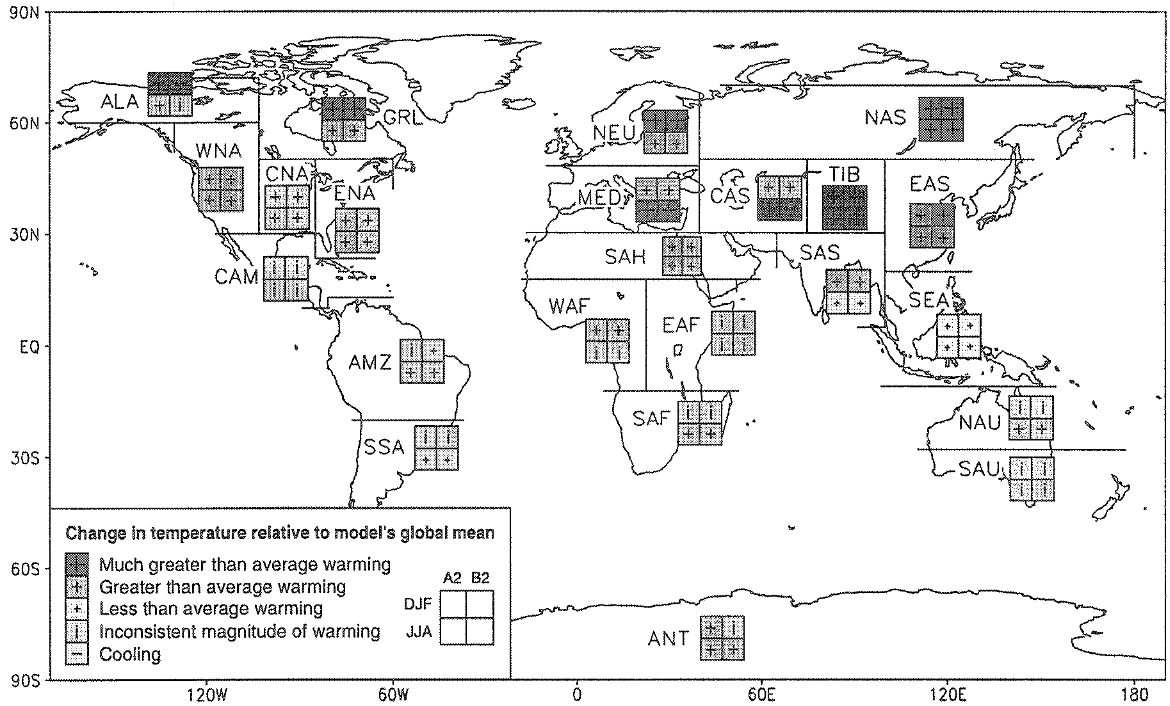

Figure 20: Analysis of inter-model consistency in regional relative warming (warming relative to each model's global-average warming). Regions are classified as showing either agreement on warming in excess of 40% above the global average ('Much greater than average warming'), agreement on warming greater than the global average ('Greater than average warming'), agreement on warming less than the global average ('Less than average warming'), or disagreement amongst models on the magnitude of regional relative warming ('Inconsistent magnitude of warming'). There is also a category for agreement on cooling (which never occurs). A consistent result from at least seven of the nine models is deemed necessary for agreement. The global annual average warming of the models used span 1.2 to 4.5°C for A2 and 0.9 to 3.4°C for B2, and therefore a regional 40% amplification represents warming ranges of 1.7 to 6.3°C for A2 and 1.3 to 4.7°C for B2. [Based on Chapter 10, Box 1, Figure 1.]

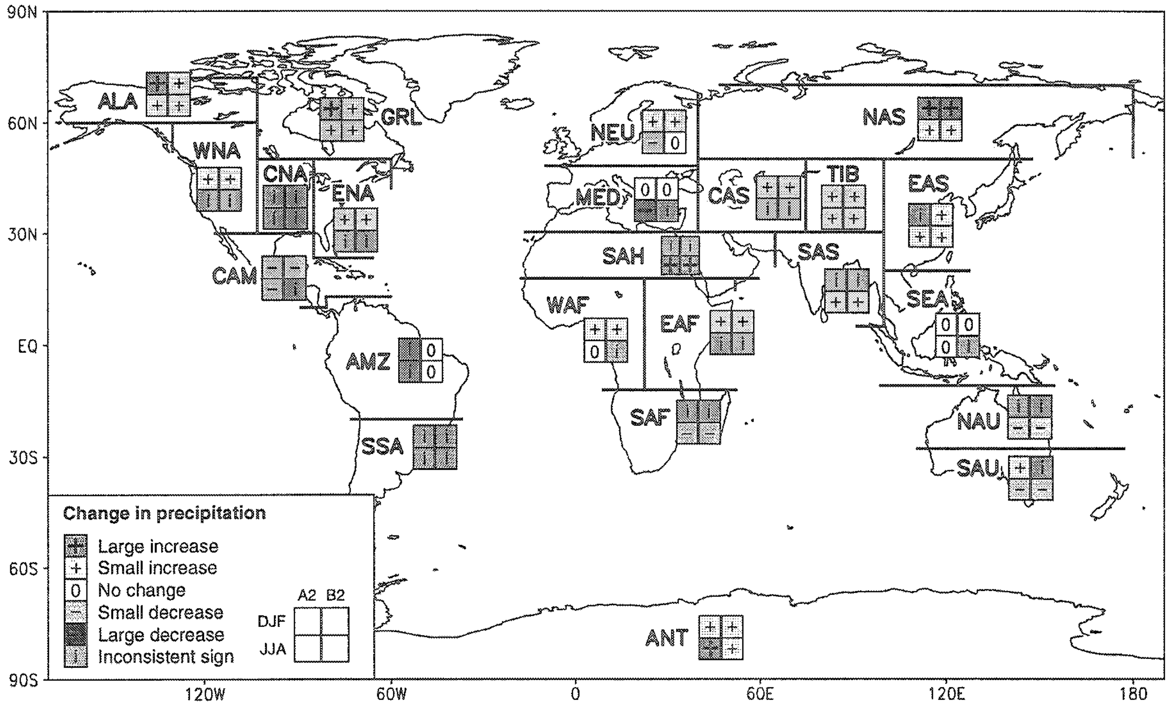

Figure 22: Analysis of inter-model consistency in regional precipitation change. Regions are classified as showing either agreement on increase with an average change of greater than 20% ('Large increase'), agreement on increase with an average change between 5 and 20% ('Increase'), agreement on a change between –5 and +5% or agreement with an average change between –5 and 5% ('No change'), agreement on decrease with an average change between –5 and -20% ('Decrease'), agreement on decrease with an average change of less than -20% ('Large decrease'), or disagreement ('Inconsistent sign'). A consistent result from at least seven of the nine models is deemed necessary for agreement. [Based on Chapter 10, Box 1, Figure 2.]

4. Projected climate change

At the global scale

- Greenhouse gases concentrations (CO_2, CH_4, N_2O) have increased since 1750 (31%, 151%, 17%).

- The similarity between climate numerical simulations of the past century and last decades observations increases when greenhouse gases and aerosols concentrations are taken into account.

- « There is new and stronger evidence that most of the warming observed over the last 50 years is attributable to human activities» (IPCC, 2001).

- Climate change projections from the models give an increase of global average surface temperature from 1,4°C to 5,8°C over the period 1990 to 2100.

- The range of these projections comes from the range of climate sensitivity simulated by the models and from the range of the emission scenarios, particularly aerosols.

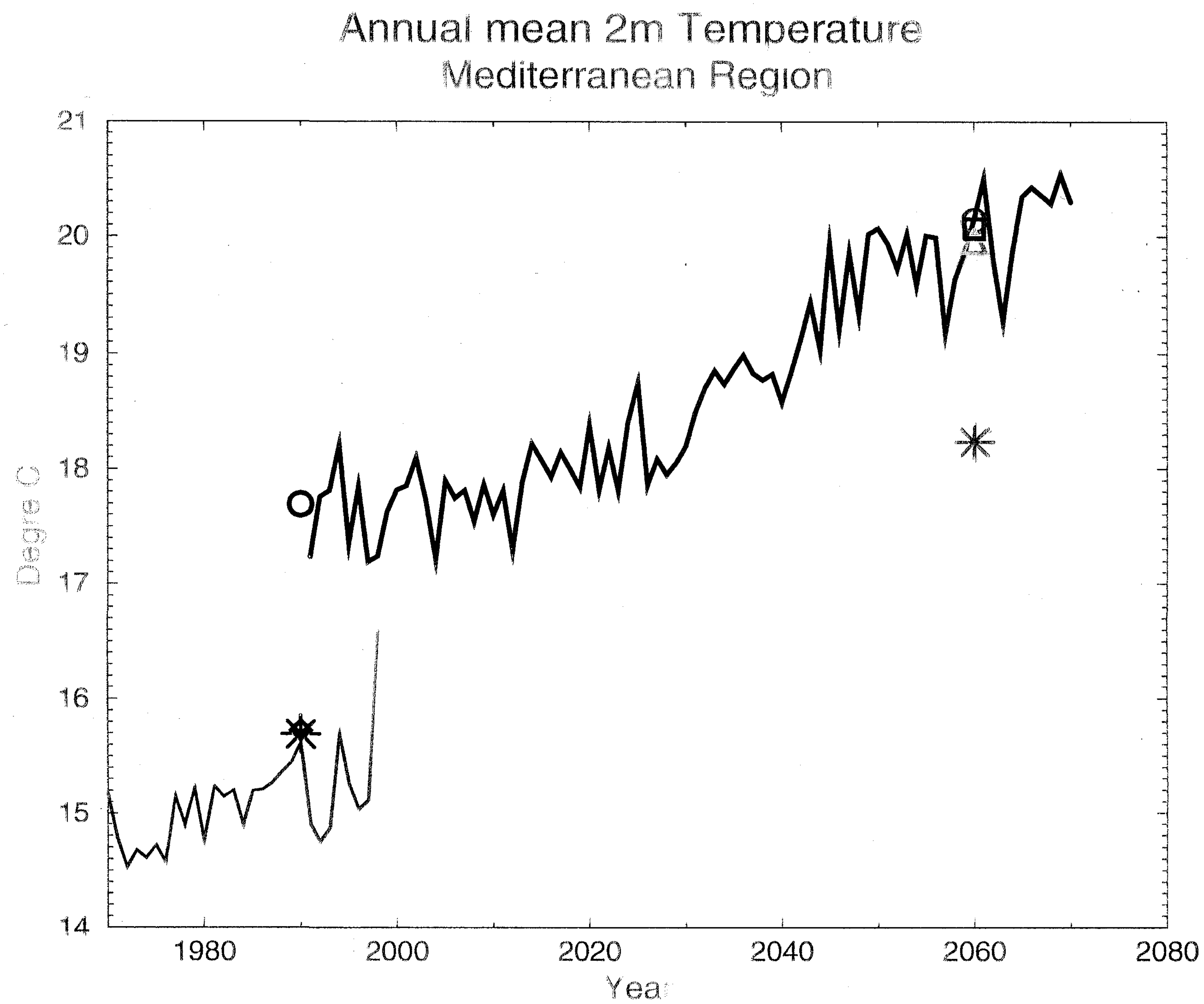
Annual mean 2m Temperature
Mediterranean Region
Degre C
21
20
19
18
17
16
15
14
1980
2000
2020
2040
2060
2080
Year

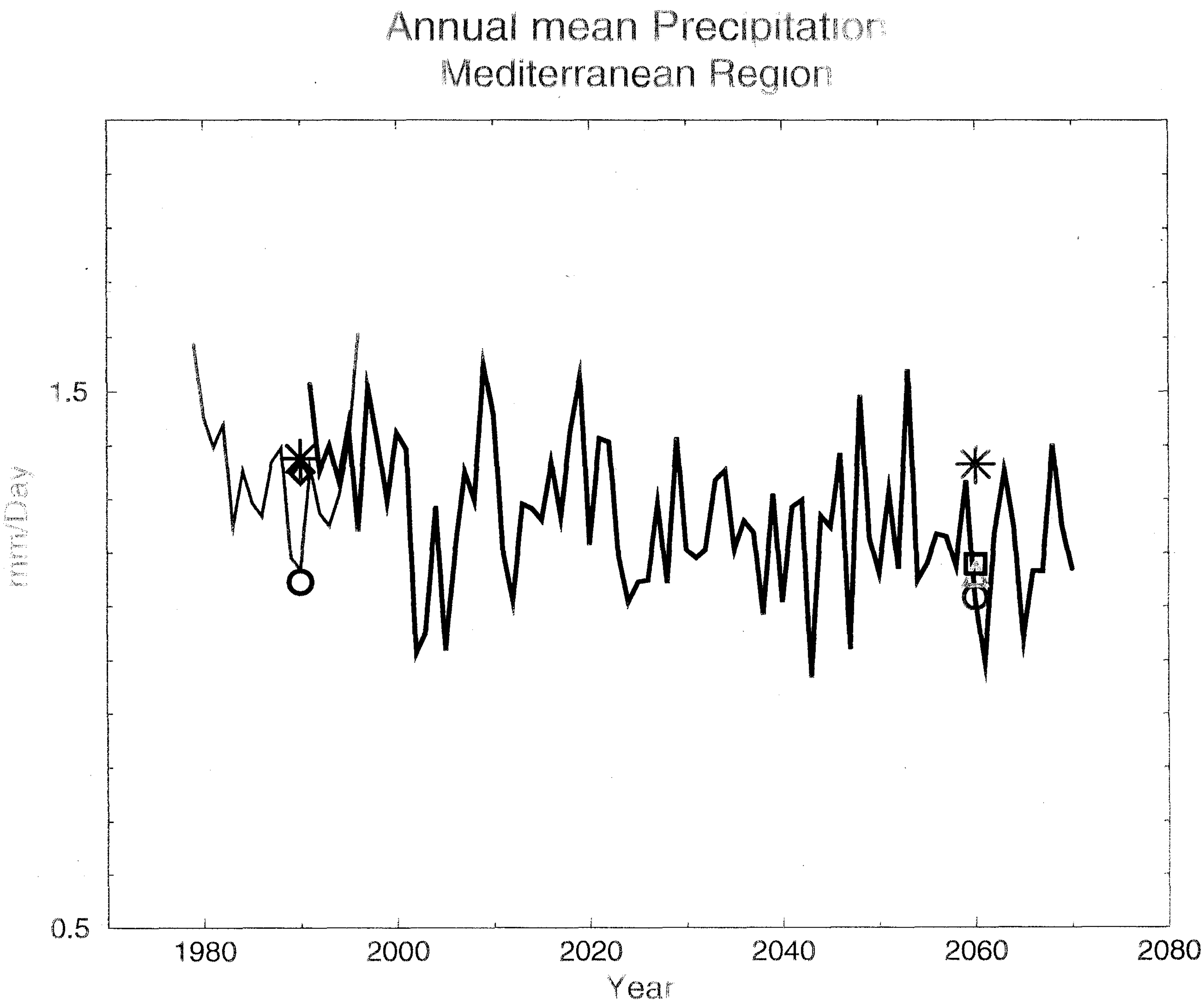
Annual mean Precipitation
Mediterranean Region
mm/Day
1.5
0.5
1980
2000
2020
2040
2060
2080
Year

2CO2−CO2 Precipitations DJF (mm/day)

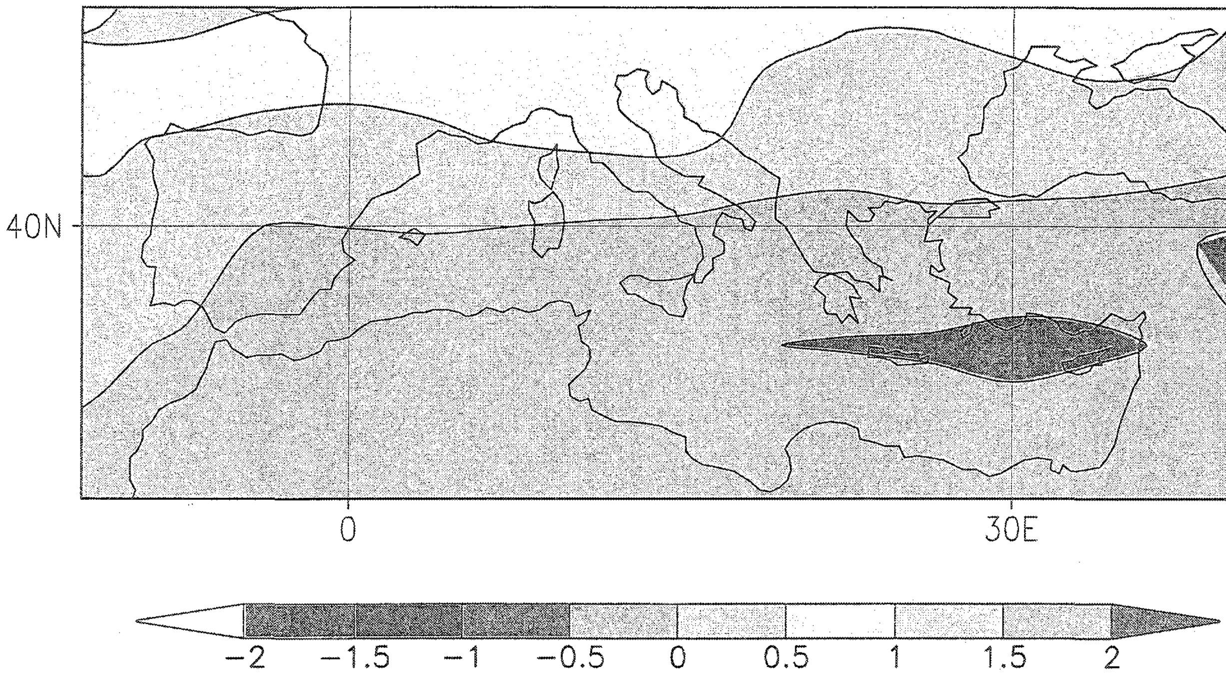

2CO2−CO2 Precipitations JJA (mm/day)

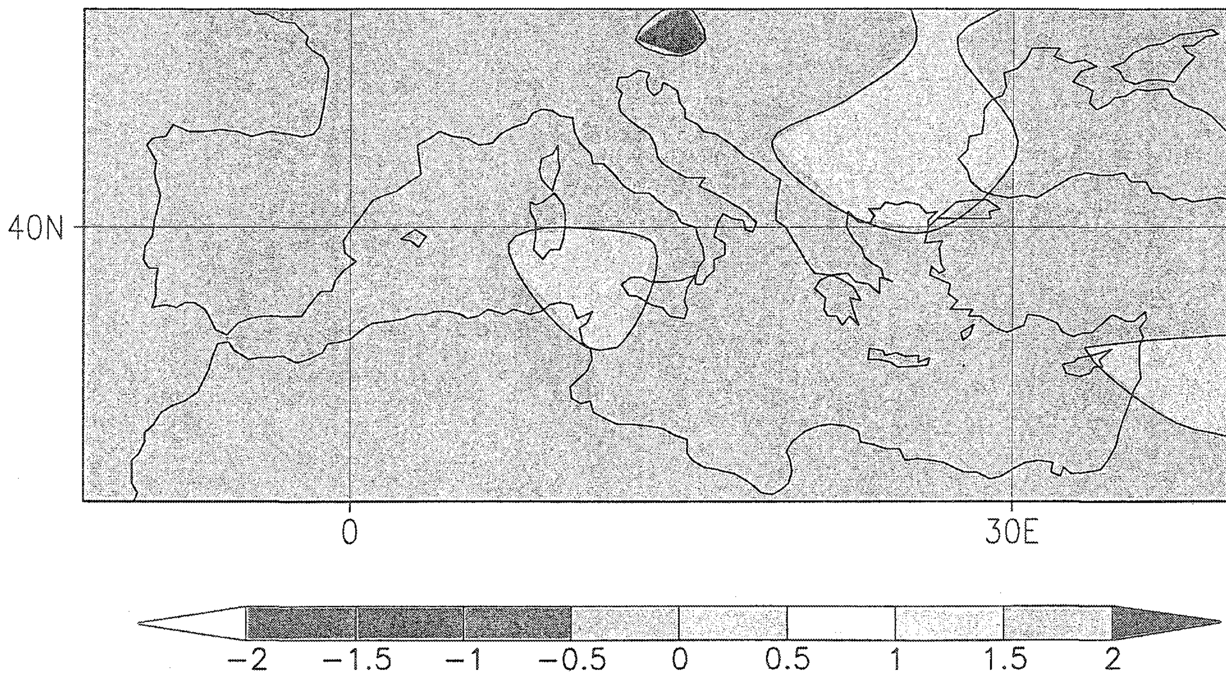

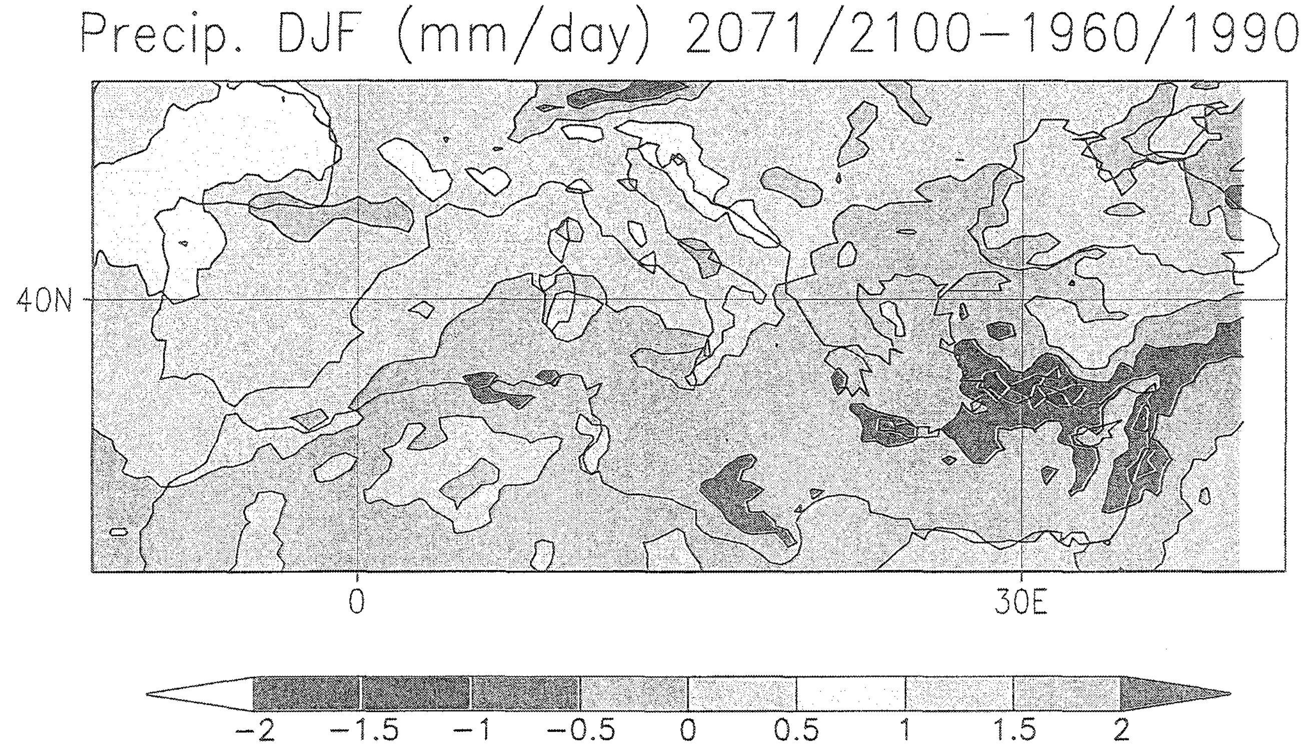
Precip. DJF (mm/day) 2071/2100-1960/1990
40N
0
30E
-2
-1.5
-1
-0.5
0
0.5
1
1.5
2

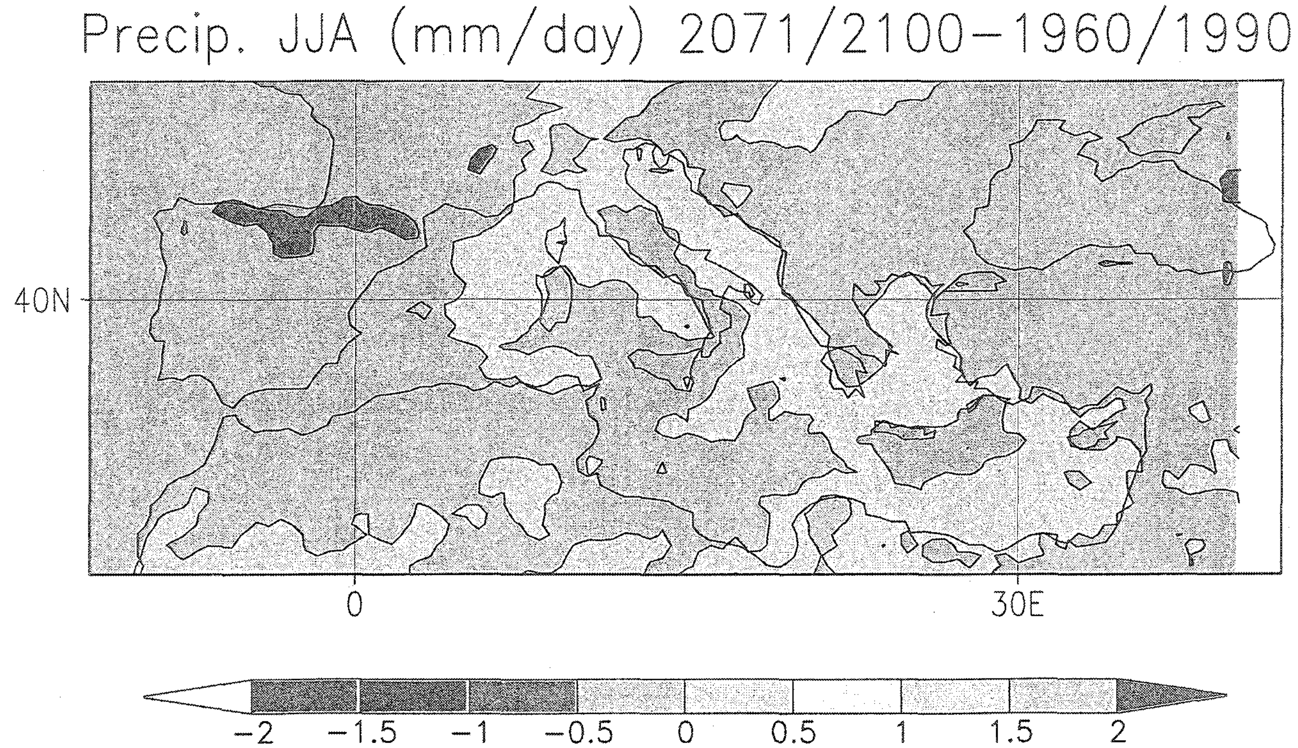
Precip. JJA (mm/day) 2071/2100-1960/1990
40N
0
30E
-2
-1.5
-1
-0.5
0
0.5
1
1.5
2

2CO2−CO2 Temperature DJF (deg.C)

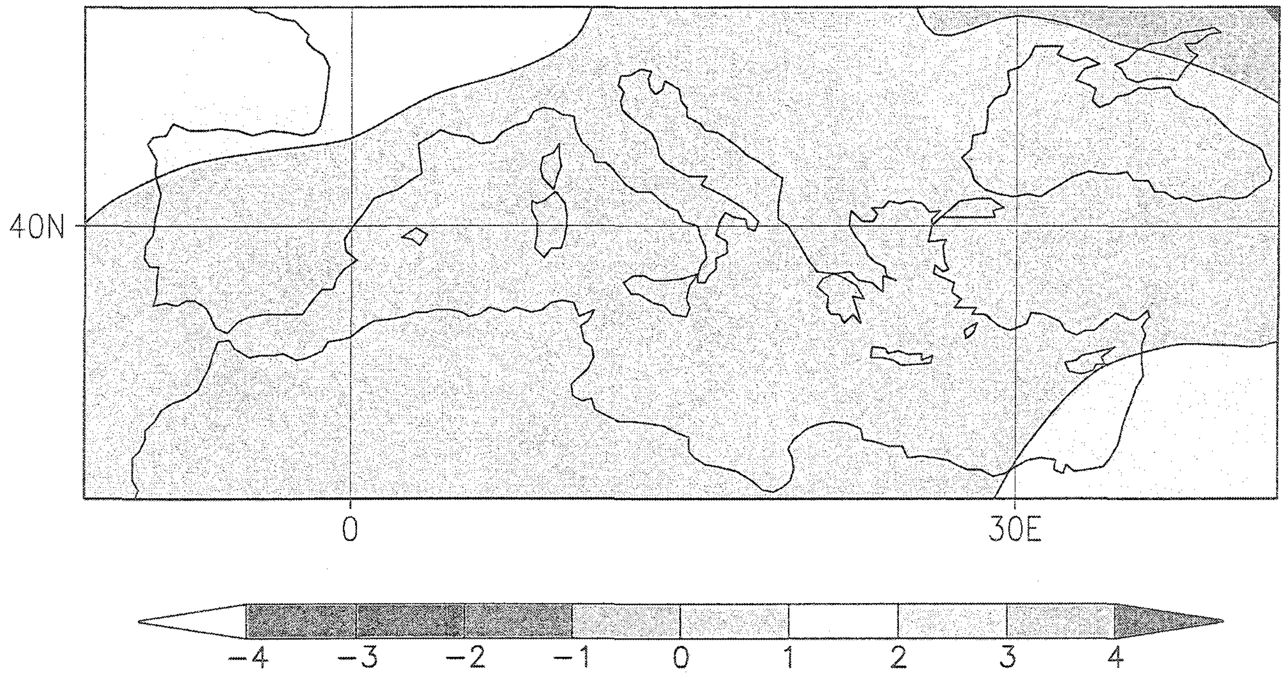

2CO2−CO2 Temperature JJA (deg.C)

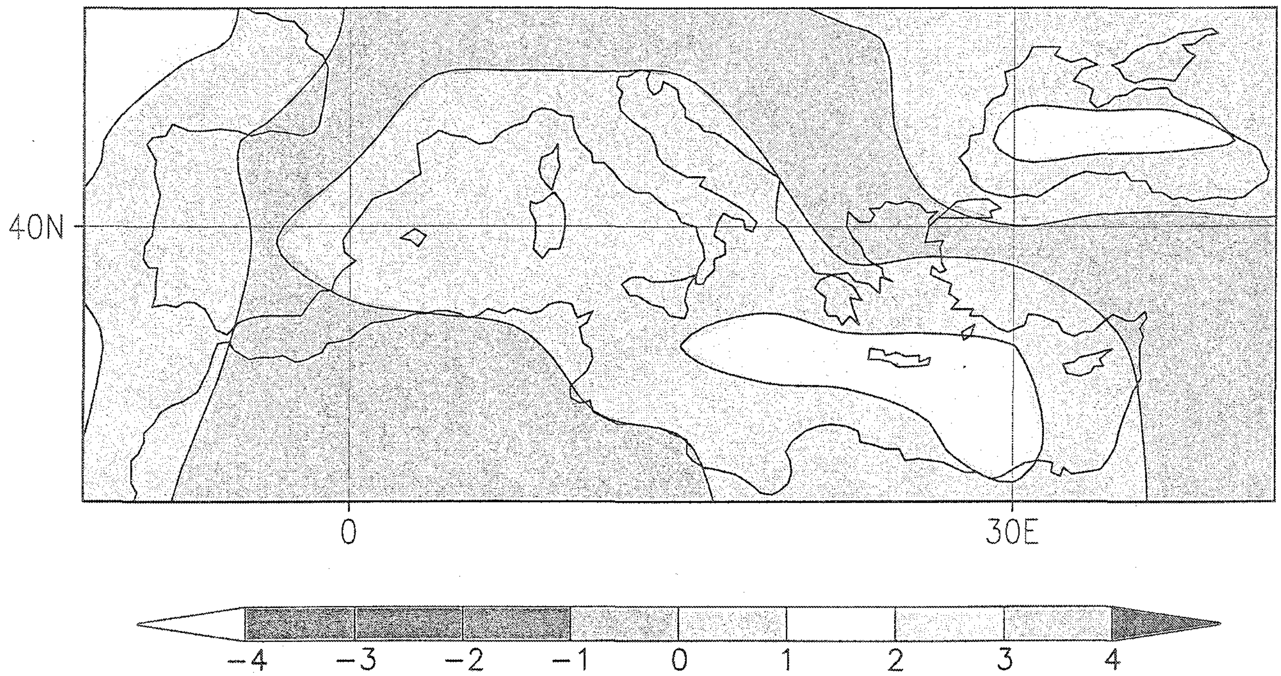

Temp.2m DJF (deg.) 2071/2100-1960/1990

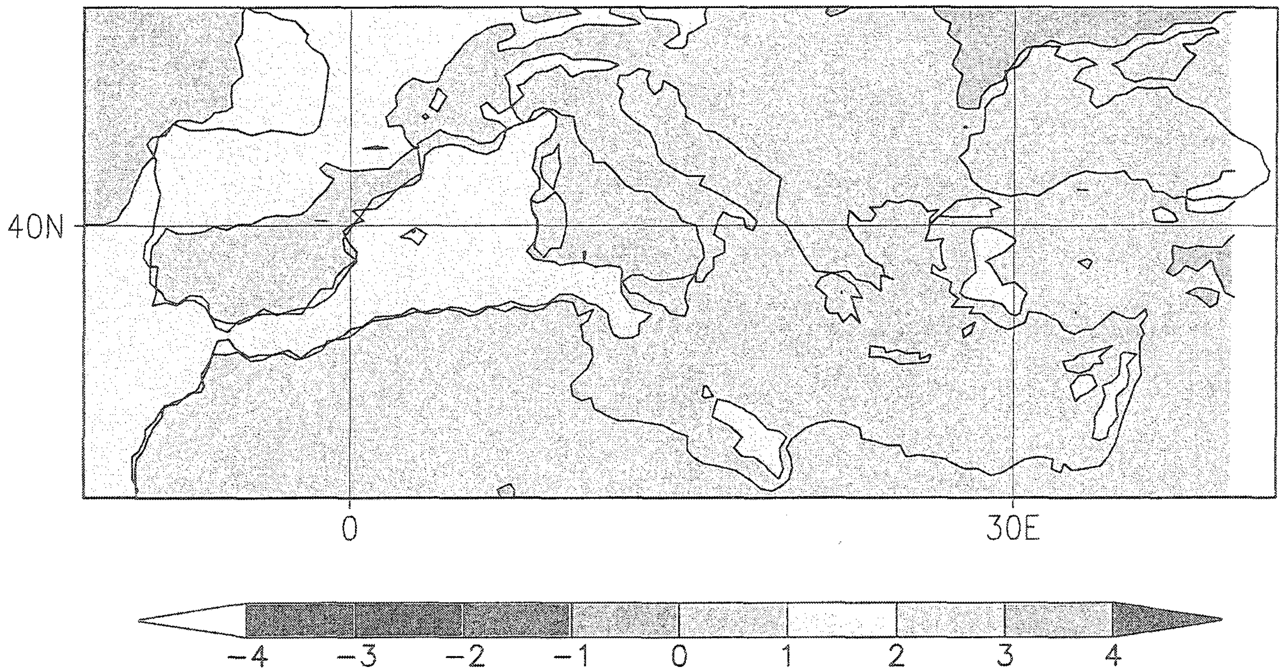

Temp.2m JJA (deg.) 2071/2100-1960/1990

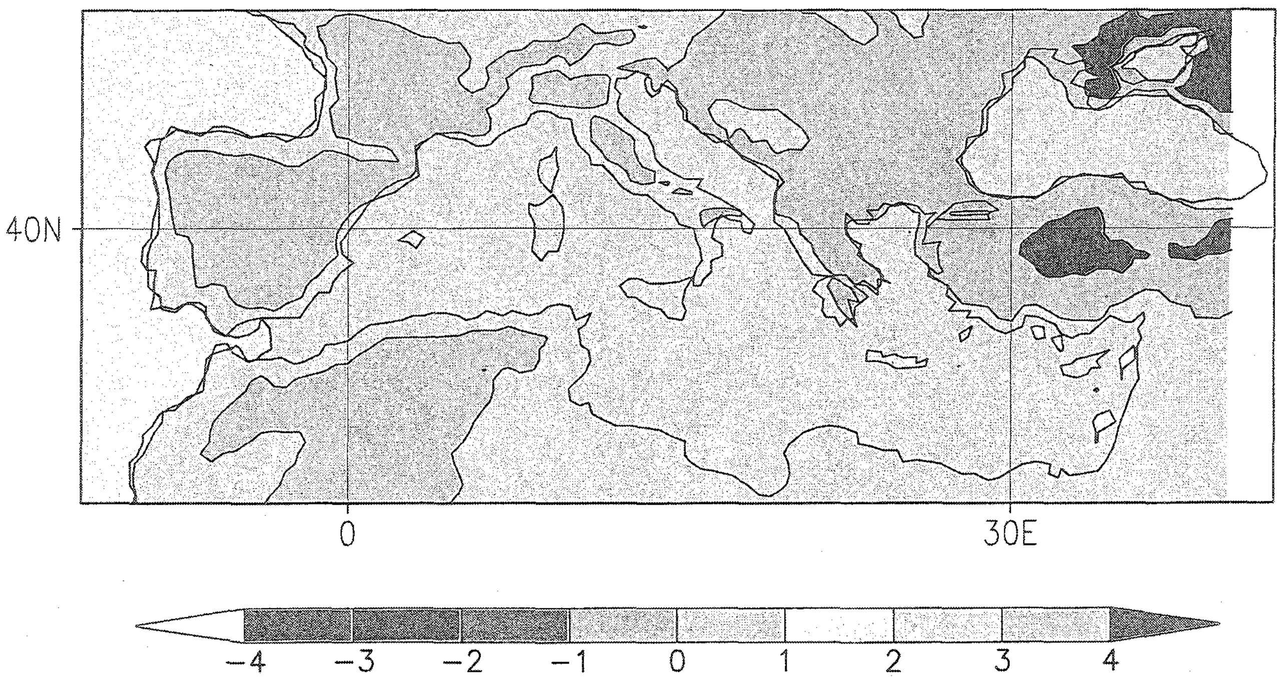

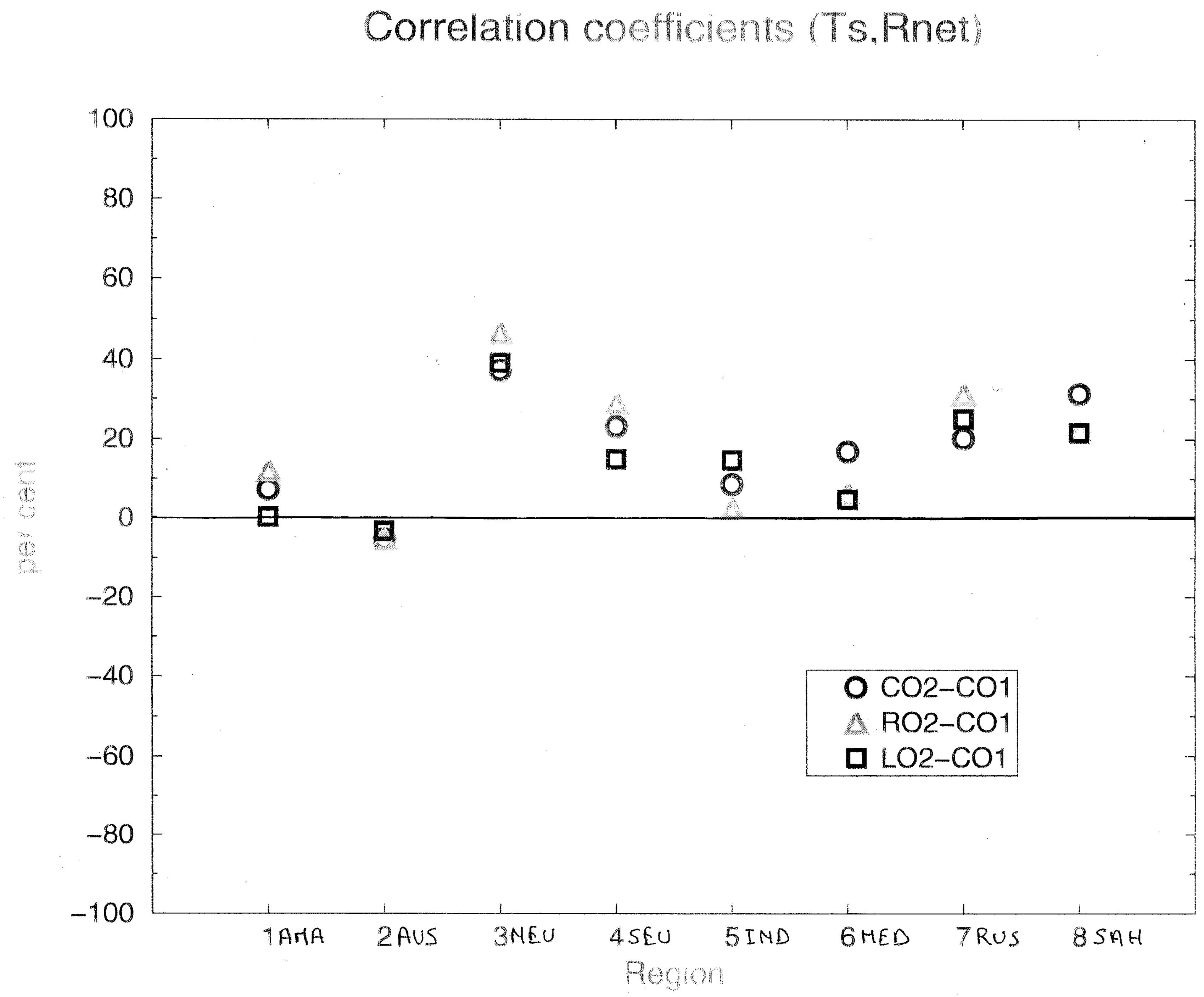
Correlation coefficients (Ts,Rnet)
100
80
60
40
20
0
−20
−40
−60
−80
−100
per cent
1AMA
2AUS
3NEU
4SEU
5IND
6MED
7RUS
8SAH
Region
CO2−CO1
RO2−CO1
LO2−CO1

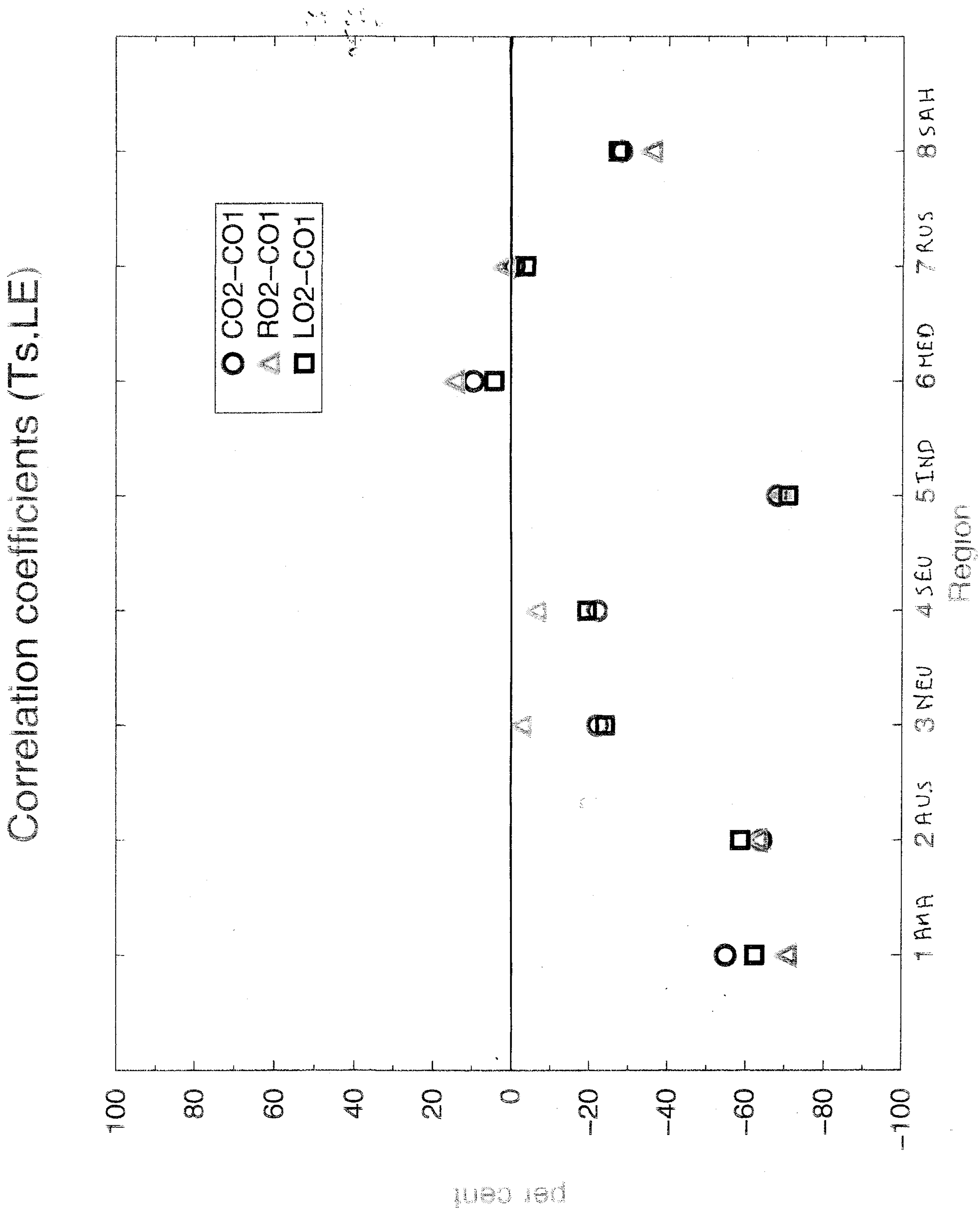
Correlation coefficients (Ts,LE)
CO2–CO1
RO2–CO1
LO2–CO1
per cent
100
80
60
40
20
0
−20
−40
−60
−80
−100
Region
1 AMA
2 AUS
3 NEU
4 SEU
5 IND
6 MED
7 RUS
8 SAH

Changes over The Mediterranean basin induced by CO2 doubling

Temperature	Western	Eastern
Winter	+2.0°C / +2.4°C	+2.3°C / +2.7°C
Summer	+2.5°C / +2.9°C	+2.3°C / +2.7°C

Precipitation	Western	Eastern
Winter	-8% / +20%	-1% / +13%
Summer	-19% / -1%	-28% / -14%

Changes over the Mediterranean basin induced by CO2 increasing at 1%/year rate

Mean for 2070-2100 minus mean for 1961-1990

Temperature	Without sulfate aerosols	With sulfate aerosols
Winter	+3.9°C / +5.3°C	+3.1°C / +4.9°C
Summer	+4.0°C / +6.9°C	+3.3°C / +5.5°C

Precipitation	Without sulphate aerosols	With sulphate aerosols
Winter	-10% / +16%	-7% / +15%
Summer	-37% / +6%	-33% / -3%

4. Projected climate change

Over the Mediterranean area

- The simulated warming due to the doubling of CO_2, is of the order of 2.4°C over the Mediterranean basin whatever the experiment and the model resolution. The simulated precipitation are rather stable or slightly decrease. This is consistent with recent observations.

- The simulated warming is greater in summer and on the Western part of the Mediterranean basin : this is consistent with the observations of 1981-1990 compared to 1951-1980.

- The simulated precipitation tends to increase in winter and to decrease in summer : consistent with observations but only for the last decade.

- Neither the hydrological control, nor the radiative control dominates the temperature anomalies. However, an analysis of the ensemble of the LSPCR simulations over Southern Europe (European research project), suggests that the seasonal dependence of the warming could be due to the seasonal dependence of the hydrological control .

4. Projected climate change

Over the Mediterranean area

- In addition to the uncertainties of emission and basis socio-economic scenarios, the uncertainty of the simulated climate change at the regional scale comes from the uncertainty of the representation of physical processes and climatic feedbacks by the models acting at the global and regional scale (clouds, aerosols, ...), the uncertainty due to the character partly chaotic of climate.